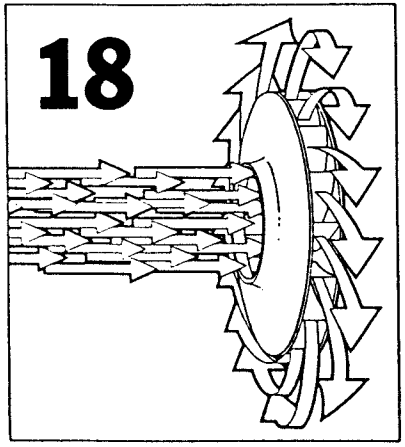

Vibration and Noise in Pumps

by **Fred R. Szenasi***
Engineering Dynamics Incorporated

Introduction

Although a certain amount of noise is to be expected from centrifugal pumps and their drivers, unusually high noise levels (in excess of 100 dB) or particularly high frequencies (whine or squeal) can be an early indicator of potential mechanical failures or vibration problems in centrifugal pumps. The purpose of this chapter is to concentrate on the mechanisms that may produce noise as a by-product; however, reduction of the noise, *per se*, is not the main concern. The main point of interest of this chapter is to study the mechanisms and their effect on the reliability of the pump system. Methods will be presented to reduce the vibration (and noise) or eliminate the basic causes by modifying the pump or piping system.

The occurrence of significant noise levels indicates that sufficient energy exists to be a potential cause of vibrations and possible damage to the pump or piping. Defining the source and cause of noise is the first step in determining whether noise is normal or whether problems may exist. Noise in pumping systems can be generated by the mechanical motion of pump components and by the liquid motion in the pump and piping systems. Noise from internal mechanical and liquid sources can be transmitted to the environment.

Effective diagnosis and treatment of noise sources to control pump noise require a knowledge of the liquid and mechanical noise-generation

* The author wishes to acknowledge the contributions by the engineering staff of Engineering Dynamics Inc., who performed many of the analyses and field tests.

mechanisms and common noise conduction paths by which noise can be transmitted. If noise itself is the major concern, it can be controlled by acoustic enclosures or other treatment [1, 2].

Sources of Pump Noise

Mechanical Noise Sources

Common mechanical sources that may produce noise include vibrating pump components or surfaces because of the pressure variations that are generated in the liquid or air. Impeller or seal rubs, defective or damaged bearings, vibrating pipe walls, and unbalanced rotors are examples of mechanical sources.

In centrifugal machines, improper installation of couplings often causes mechanical noise at twice pump speed (misalignment). If pump speed is near or passes through the lateral critical speed, noise can be generated by high vibrations resulting from imbalance or by the rubbing of bearings, seals, or impellers. If rubbing occurs, it may be characterized by a high-pitched squeal. Windage noises may be generated by motor fans, shaft keys, and coupling bolts. Damaged rolling element bearings produce high-frequency noise [3] related to the bearing geometry and speed.

Liquid Noise Sources

These are pressure fluctuations produced directly by liquid motion. Liquid noise can be produced by vortex formation in high-velocity flow (turbulence), pulsations, cavitation, flashing, water hammer, flow separation, and impeller interaction with the pump cutwater. The resulting pressure pulsations and flow modulations may produce either a discrete or broad-band frequency component. If the generated frequencies excite any part of the structure including the piping or the pump into mechanical vibration, then noise may be radiated into the environment. Four types of pulsation sources occur commonly in centrifugal pumps [2]:

- Discrete-frequency components generated by the pump impeller such as vane passing frequency and multiples.
- Flow-induced pulsation caused by turbulence such as flow past restrictions and side branches in the piping system.
- Broad-band turbulent energy resulting from high flow velocities.
- Intermittent bursts of broad-band energy caused by cavitation, flashing, and water hammer.

A variety of secondary flow patterns [4] that produce pressure fluctuations are possible in centrifugal pumps, as shown in Figure 18-1, particularly for operation at off-design flow. The numbers shown in the flow stream are the locations of the following flow mechanisms:

1. Stall
2. Recirculation (secondary flow)
3. Circulation
4. Leakage
5. Unsteady flow fluctuations
6. Wake (vortices)
7. Turbulence
8. Cavitation

Causes of Vibrations

Causes of vibrations are of major concern because of the damage to the pump and piping that generally results from excessive vibrations. Vibrations in pumps may be a result of improper installation or maintenance,

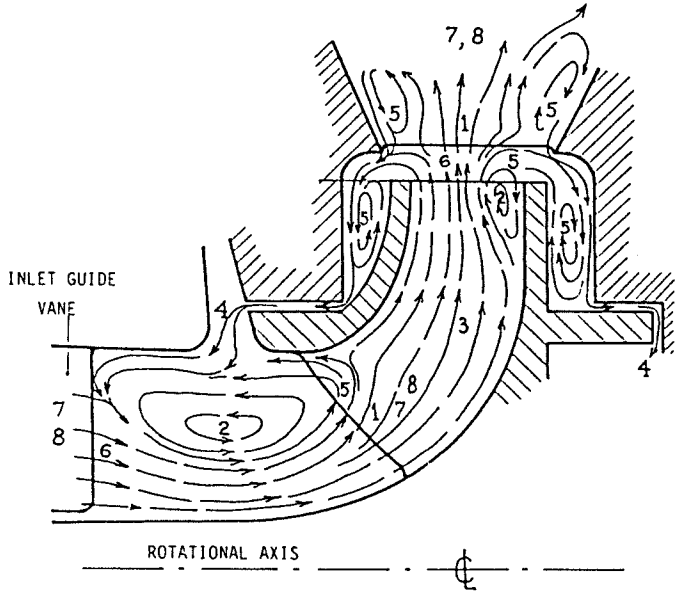

Figure 18-1. Secondary flow around pump impeller off-design flow EPRI Research Project 1266-18, Report CS-1445 [4].

incorrect application, hydraulic interaction with the piping system, or design and manufacturing flaws. Some of the common causes of excessive vibrations and failures are [5]:

Installation/Maintenance

Unbalance
Shaft-to-shaft misalignment
Seal rubs
Case distortion caused by piping loads
Piping dynamic response (supports and restraints)
Support structural response (foundation)
Anchor bolts/grout
Improper assembly

Application

Operating off of design point
Improper speed/flow
Inadequate NPSH
Entrained air

Hydraulic

Interaction of pump (head-flow curve) with piping resonances
Hydraulic instabilities
Acoustic resonances (pressure pulsations)
Water hammer
Flow distribution problems
Recirculation
Cavitation
Flow induced excitation (turbulence)
High flow velocity

Design/Manufacturing

Lateral critical speeds
Torsional critical speeds
Improper bearings or seals
Rotor instability
Shaft misalignment in journals
Impeller resonances
Bearing housing/pedestal resonances

Many of these causes are a result of an interaction of the pump (or its driver) with the fluid or the structure (including piping). This interactive relationship requires that the complete system be evaluated rather than investigating individual components when problems occur. Although prototype pumps or a new design may run the gambit of these problems, standard design or "off-the-shelf" pumps are not immune, particularly to system problems.

Installation/Maintenance Effects

Unbalance. Unbalance of a rotating shaft can cause large transverse vibrations at certain speeds, known as critical speeds, that coincide with the lateral natural frequencies of the shaft. Lateral vibration due to unbalance is probably the most common cause of downtime and failures in centrifugal pumps. Damage due to unbalance response may range from seal or bearing wipes to catastrophic failures of the rotor. Excessive unbalance can result from rotor bow, unbalanced couplings, thermal distortion, or loose parts. All too often, field balancing is required even after careful shop balancing has been performed.

Although a pump rotor may be adequately balanced at startup, after a period of operation the pump rotor may become unbalanced by erosion, corrosion, or wear. Unbalance could also be caused by non-uniform plating of the pumped product onto the impeller. In this instance, cleaning the impeller could restore the balance. Erosion of the impeller by cavitation or chemical reaction with the product may cause permanent unbalance requiring replacement of the impeller. Wear of the impeller or shaft caused by rubs will require the repair or replacement of the damaged component. Another cause of unbalance can occur if lubricated couplings have an uneven build-up of grease or sludge.

Assembly or manufacturing procedures may cause a new pump rotor to be unbalanced because of slight manufacturing imperfections or tolerance build-up resulting in the center of mass of the rotor not being exactly at the center of rotation. Forging or casting procedures can produce local variations in the density of the metal due to inclusions or voids. On large cast impellers, the bore for the shaft may not be exactly centered with the casting geometry. Stacking a rotor can result in thermal distortions of the shaft or impellers that can result in a cocked impeller. Nonsymmetries of just a few mils caused by these manufacturing or assembly methods can result in significant forces generated by a high speed rotor. Most of these nonsymmetries can be compensated for by balancing the rotor.

Misalignment. Angular misalignment between two shafts connected with a flexible coupling introduces an additional driving force that can

produce torsional or lateral vibrations. The forces in a typical industrial coupling are similar to those in a universal joint (Figure 18-2). When a small angular misalignment occurs, the velocity ratio across the joint is not constant. If one shaft speed is assumed constant, then the other shaft has a faster rotational rate [6] for part of the revolution and a slower rotational rate for part of the revolution. This variation of rotating speed results in a second harmonic (twice shaft speed) vibrational component.

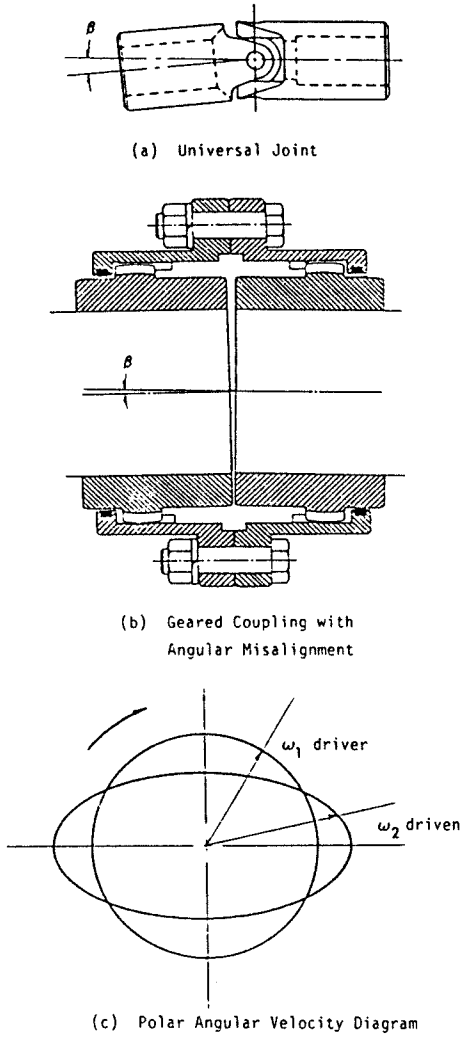

Figure 18-2. Effects of angular misalignment in shaft couplings.

Piping and Structure. The pump should be relatively isolated from the piping. The weight and thermal loading on the suction and discharge connections should be minimized. The American Petroleum Institute (API) Standard 610 [7] specifies allowable external nozzle forces and moments. Most pump manufacturers specify allowable weight and thermal loads transferred from the pipe to the pump case. Static forces from the piping may misalign the pump from its driver, or for excessive loading, the pump case may become distorted and cause rubs or seal and bearing damage. Thermal flexibility analyses of the piping should be performed to evaluate piping loads and to design the necessary supports and restraints to minimize the transfer of piping loads to the operating equipment.

Vibrations of the piping or the support structure can be mechanically transferred to the pump. The piping and the structure should not have their resonant frequencies coincident with any of the pump excitations such as vane passing frequency or multiples. The vibrations transferred from the pipe to the structure can be minimized by using a visco-elastic material (i.e., belting material) between the pipe and the pipe clamp.

Application

The initial stage of pump system design should include the task of defining the range of operating conditions for pressure, flow, temperatures, and the fluid properties. The vendors can provide the correct pump geometry for these design conditions. Expected variations in operating conditions and fluid composition, if a significant percentage, may influence the design.

Improper application or changing conditions can result in a variety of problems. Operation at high-flow, low-head conditions can cause vibrations of the rotor and case. Inadequate NPSH can result in cavitation that will cause noise and vibration of varying degrees.

Bearings. General purpose, small horsepower pumps in process plants generally have rolling element bearings. Noise and vibrations are commonly a result of bearing wear. As the rolling elements or races wear, the worn surfaces or defects initially produce a noise and as wear increases vibrations may become noticeable. Several vibrational frequencies may occur that depend on the geometry of the bearing components and their relative rotational speeds [3]. The frequencies are generally above operating speed.

Many ball bearing failures [8] are due to contaminants in the lubricant that have found their way into the bearing after the machine has been placed in operation. Common contaminants include moisture, dirt, and other miscellaneous particles which, when trapped inside the bearing, may cause wear or permanently indent the balls and raceways under the tremendous stresses generated by the operating load.

Special purpose pumps and large boiler feed pumps commonly have oil film (hydrodynamic) bearings. The hydrodynamic bearing is superior to rolling element bearings for high speed or high load application. The hydrodynamic bearing supports the rotor on a film of oil as it rotates. The geometry of the hydrodynamic bearing and the oil properties play an important role in controlling the lateral critical speeds and consequently the vibrational characteristics of the pump.

Seals. The fluid dynamics of flow through seals have a dramatic effect on rotordynamics [9]. Hydrodynamic forces involved may contribute to the stabilization of rotating machinery or make it unstable. Seals with large axial flow in the turbulent range, such as in feed water pumps, tend to produce large stiffness and damping coefficients that are beneficial to rotor vibrations and stability. Wear of the seals will increase the clearance and cause greater leakage and possibly change the rotordynamic characteristics of the seal resulting in increased vibrations.

Hydraulic Effects

Hydraulic effects and pulsations can result in almost any frequency of vibration of the pump or piping from once per revolution up to the vane passing frequency and its harmonics. Frequencies below running speed can be caused by acoustical resonances. Generally, these effects are due to the impeller passing the discharge diffuser or some other discontinuity in the case. Any nonsymmetry of the internals of the pump may produce an uneven pressure distribution that can result in forces applied to the rotor.

Transients. Starting and stopping pumps with the attendant opening and closing of valves is a major cause of severe transients in piping systems. The resulting pressure surge, referred to as water hammer, can apply a sudden impact force to the pump, its internals, and the piping. Severe water hammer has caused cracks in concrete structures to which the pipe was anchored.

Rapid closure of conventional valves used in feedwater lines can cause severe water hammer. Increasing the closure time of the valve can reduce the severity of the surge pressure. Analytical methods are available to evaluate the severity of water hammer in a particular piping configuration for various closure rates [10].

Cavitation and Flashing. For many liquid pump piping systems, it is common to have some degree of flashing and cavitation associated with the pump or with the pressure control valves in the piping system. High flow rates produce more severe cavitation because of greater flow losses through restrictions.

Cavitation produces high local pressures that may be transmitted directly to the pump or piping and may also be transmitted through the fluid to other areas of the piping. Cavitation is one of the most commonly occurring and damaging problems in liquid pump systems. The term cavitation refers to the formation and subsequent collapse of vapor bubbles (or cavities) in a liquid caused by dynamic pressure variations near the vapor pressure. Cavitation can produce noise, vibration, loss of head and capacity as well as severe erosion of the impeller and casing surfaces.

Before the pressure of the liquid flowing through a centrifugal pump is increased, the liquid may experience a pressure drop inside the pump case. This is due in part to acceleration of the liquid into the eye of the impeller and flow separation from the impeller inlet vanes. If flow is in excess of design or the incident vane angle is incorrect, high-velocity, low-pressure eddies may form. If the liquid pressure is reduced to the vaporization pressure, the liquid will flash. Later in the flow path the pressure will increase. The implosion which follows causes what is usually referred to as cavitation noise. The collapse of the vapor pockets, usually on the nonpressure side of the impeller vanes, causes severe damage (vane erosion) in addition to noise.

When a centrifugal pump is operated at flows away from the point of best efficiency, noise is often heard around the pump casing. The magnitude and frequency of this noise may vary from pump to pump and are dependent on the magnitude of the pump head being generated, the ratio of NPSH required to NPSH available, and the amount by which actual flow deviates from ideal flow. Noise is often generated when the vane angles of the inlet guides, impeller, and diffuser are incorrect for the actual flow rate.

Cavitation can best be recognized by observing the complex wave or dynamic pressure variation using an oscilloscope and a pressure transducer. The pressure waveform will be non-sinusoidal with sharp maximum peaks (spikes) and rounded minimum peaks occurring at vapor pressure as shown in Figure 18-3. As the pressure drops, it cannot produce a vacuum less than the vapor pressure.

Cavitation-like noise can also be heard at flows less than design, even when available inlet NPSH is in excess of pump required NPSH, and this has been a puzzling problem. An explanation offered by Fraser [11, 12] suggests that noise of a very low, random frequency but very high intensity results from backflow at the impeller eye or at the impeller discharge, or both. Every centrifugal pump has this recirculation under certain conditions of flow reduction. Operation in a recirculating condition can be damaging to the pressure side of the inlet and/or discharge impeller vanes (and also to casing vanes). Recirculation is evidenced by an increase in loudness of a banging type, random noise, and an increase in suction and/or discharge pressure pulsations as flow is decreased.

Sound levels measured at the casing of an 8000 hp pump and near the suction piping during cavitation [2] are shown in Figure 18-4. The cavitation produced a wide-band shock that excited many frequencies; however, in this case, the vane passing frequency (number of impeller vanes

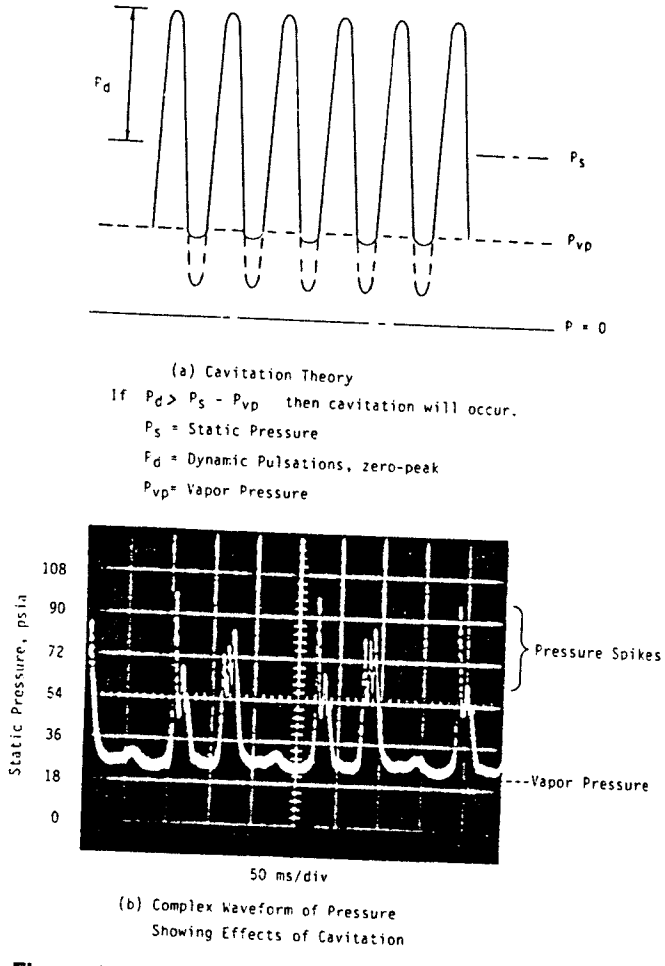

Figure 18-3. Cavitation effects on the dynamic pressure.

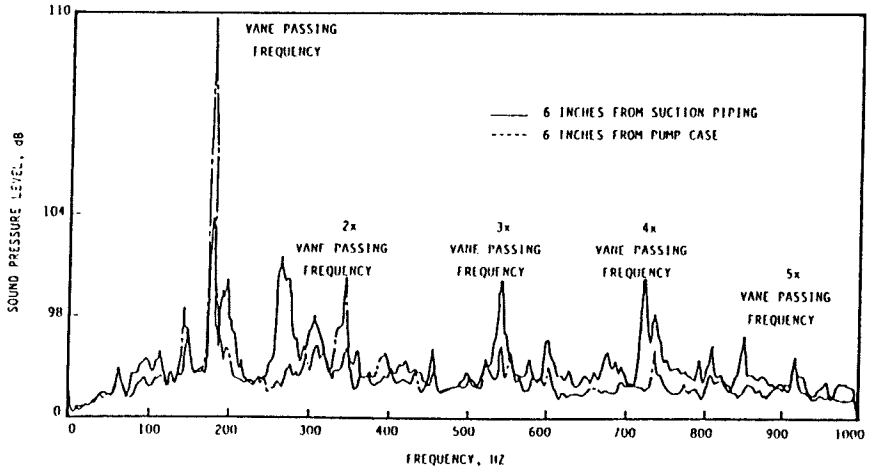

Figure 18-4. Noise spectra of cavitation in centrifugal pump.

times revolutions per second) and multiples of it predominated. Cavitation noise of this type usually produces very high frequency noise, best described as "crackling."

Flashing is particularly common in hot water systems (feedwater pump systems) when the hot, pressurized water experiences a decrease in pressure through a restriction (i.e., flow control valve). This reduction of pressure allows the liquid to suddenly vaporize, or flash, which results in a noise similar to cavitation. To avoid flashing after a restriction, sufficient back pressure should be provided. Alternately, the restriction could be located at the end of the line so that the flashing energy can dissipate into a larger volume.

Flow Turbulence. Pump generated dynamic pressure sources include turbulence (vortices or wakes) produced in the clearance space between impeller vane tips and the stationary diffuser or volute lips. Dynamic pressure fluctuations or pulsations produced in this manner can cause impeller vibrations or can result in shaft vibrations as the pressure pulses impinge on the impeller.

Flow past an obstruction or restriction in the piping may produce turbulence or flow-induced pulsations [2]. These pulsations may produce both noise and vibration over a wide-frequency band. The frequencies are related to the flow velocity and geometry of the obstruction. These pulsations may cause a resonant interaction with other parts of the acoustic piping system.

Most of these unstable flow patterns are produced by shearing at the boundary between a high-velocity and low-velocity region in a fluid

field. Typical examples of this type of turbulence include flow around obstructions or past deadwater regions (i.e., a closed bypass line) or by bi-directional flow. The shearing action produces vortices, or eddies that are converted to pressure perturbations at the pipe wall that may result in localized vibration excitation of the piping or pump components. The acoustic natural response modes of the piping system and the location of the turbulence has a strong influence on the frequency and amplitude of this vortex shedding. Experimental measurements have shown that vortex flow is more severe when a system acoustic resonance coincides with the generation frequency of the source. The vortices produce broad-band turbulent energy centered around a frequency that can be determined with a dimensionless Strouhal number (S_n) from 0.2 to 0.5, where

$$f = \frac{S_n V}{D}$$

where f = vortex frequency, Hz
S_n = Strouhal number, dimensionless (0.2 to 0.5)
V = flow velocity in the pipe, ft/sec
D = a characteristic dimension of the obstruction, ft

For flow past tubes, D is the tube diameter, and for excitation by flow past a branch pipe, D is the inside diameter of the branch pipe. The basic Strouhal equation is further defined in Table 18-1, items 2A and 2B. As an example, flow at 100 ft/sec past a 6-inch diameter stub line would produce broad-band turbulence at frequencies from 40 to 100 Hz. If the stub were acoustically resonant to a frequency in that range, large pulsation amplitudes could result.

Pressure regulators or flow control valves may produce noise associated with both turbulence and flow separation. These valves, when operating with a severe pressure drop, have high-flow velocities which generate significant turbulence. Although the generated noise spectrum is very broad-band, it is characteristically centered around a frequency corresponding to a Strouhal number of approximately 0.2.

Pulsations. Pumping systems produce dynamic pressure variations or pulsations through normal pumping action. Common sources of pulsations occur from mechanisms within the pump. The pulsation amplitudes in a centrifugal pump are generated by the turbulent energy that depends upon the clearance space between impeller vane tips and the stationary diffuser or volute lips, the installed clearances of seal, wear rings and the symmetry of the pump rotor and case. Because these dimensions are not accurately known, predicting the pulsation amplitudes is difficult. Even identical pumps often have different pressure pulsation amplitudes.

Table 18-1
Pulsation Sources

Generation Mechanism	Excitation Frequencies	
1. Centrifugal Compressors & Pumps	$f = \frac{nN}{60}$	
	$f = \frac{nBN}{60}$	B = Number of Blades
	$f = \frac{nvN}{60}$	v = Number of Volutes or Diffuser Vanes
2. Flow Excited		
A. Flow through Restrictions or Across Obstructions	$f = S\frac{V}{D}$	S = Strouhal Number = .2 to .5 V = Flow Velocity, ft/sec D = Restriction diameter, ft
B. Flow Past Stubs	$f = S\frac{V}{D}$	S = .2 to .5
C. Flow Turbulence Due to Quasi Steady Flow	$f = 0 - 30$ Hz (Typically)	
D. Cavitation and Flashing	Broad Band	

Even with the pump operating at its best efficiency point and proper conditions (NPSH, etc.) pulsations may be generated by high-flow velocities and turbulence at the vane tips or at the cutwater. As operating conditions deviate from the design conditions, more sources may come into play such as cavitation, recirculation, flow instabilities, etc.

These pulsations can interact with the hydraulic or acoustic natural frequencies of the piping system to amplify the pulsation. Acoustic natural frequencies in piping systems are a function of the fluid properties, the piping, and pump geometry. The acoustic interaction can be compared to the action of an organ pipe resonance where turbulence produced at the lip is amplified into an audible tone. Similarly, pulsations from the pump are amplified into pressure pulsations that react at elbows, restrictions, closed valves, and piping size changes to cause dynamic shaking forces. This conversion of hydraulic energy into mechanical forces can result in vibrations of the pump, piping, and their support structure.

In the design stage, the acoustical natural frequencies of piping systems can be calculated using either digital [13] or analog [14] modeling

procedures. As an example, a model of a piping system analyzed by a digital acoustic analysis technique is given in Figure 18-5. The system was for chemical service with three pumps (3000 gpm, 250 psi, 3600 rpm) each 50% capacity (one spare). The predicted frequency response in the pump system at selected locations is given in Figure 18-6. The natural frequencies of the energy in the piping system can be compared to discrete frequencies generated by the pump (i.e., vane passing frequency, etc). It can immediately be seen that these 3600 rpm pumps (A and B operating) with a six-vane impeller could cause severe pulsations in the piping system because its vane passing frequency (6 × 60 rps) matches an acoustic response at 360 Hz. Based on the acoustic analysis, a seven-vane impeller should be used that would have its vane passing frequency at 420 Hz (7 × 60 rps) which has minimal response.

While in the design stage, changing the pump impeller for this system was a simple solution; however, the primary use of this acoustic analysis technique is to evaluate alternate piping configurations when the pump cannot be readily changed as in existing installations. Modifications to the piping system (i.e., lengths, routing) can be easily simulated to evaluate the effectiveness in attenuating a particular response mode.

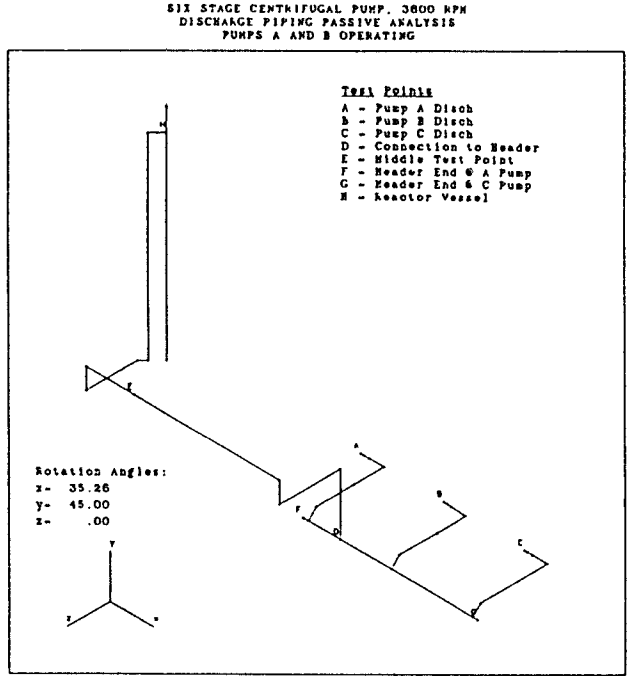

Figure 18-5. Simulation of centrifugal pump piping system.

The mechanical natural frequencies of the piping spans should not occur in the same range as the acoustic response frequencies. The analysis aids in determining the allowable frequency range that can be used to establish the proper design of the piping supports and span lengths to minimize the potential for exciting a piping resonance. The acoustic analysis can be used to redesign the piping to modify the frequency response and particular acoustic modes that may be predominant.

Acoustic Resonance. When a dynamic pressure pulse propagates down a pipe and reaches a restriction or pipe size change (flow area), the pulse is reflected [13, 15]. As the series of pressure pulses continue to be reflected, a standing wave is generated; that is, at a point in the pipe, the pressure periodically rises above and drops below the average line pressure (simple harmonic variation). The super-position of an incident pulse and a reflected pulse, being the sum of two pulses traveling in opposite directions, produce the standing wave.

If the timing (phasing) of a reflected pulse matches a new pulse, the two pulses will add, or amplify. The timing of the pulses are dependent

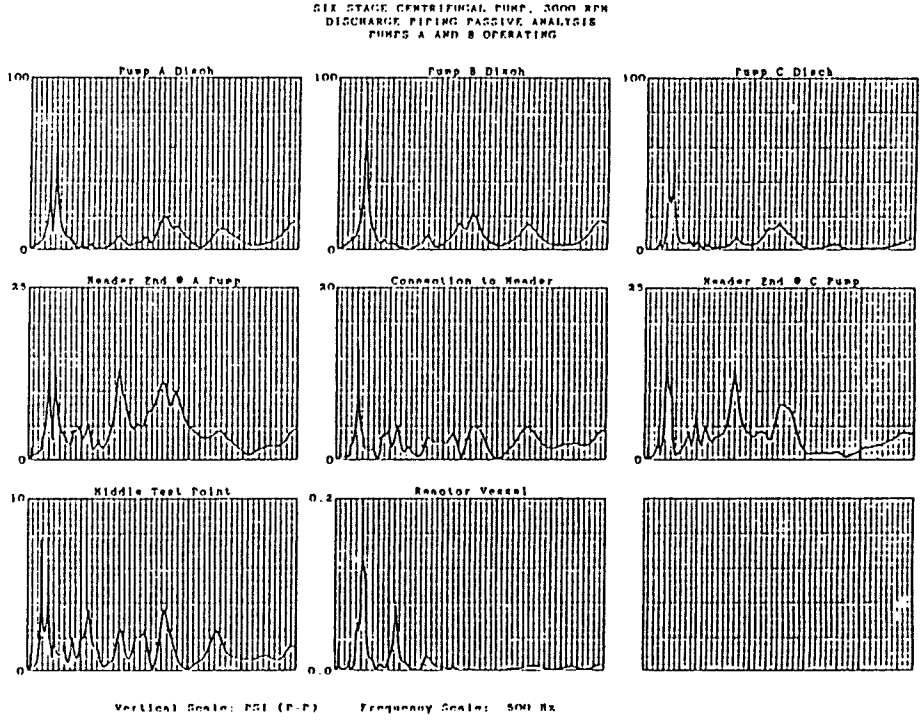

Figure 18-6. Passive acoustic response of piping system.

upon the pump speed (frequency) and pipe length (distance traveled) and the physical properties of the fluid.

The acoustic velocity, a function of the fluid density and bulk modulus, is an important factor in determining the resonant frequency of a pipe length. The API has published a comprehensive handbook for the physical properties of hydrocarbon gasses and liquids [16]. Calculation procedures for the acoustic velocity of water and other common liquids are presented in the Appendix at the end of this chapter.

A resonant condition [17] exists when the standing wave amplitude is reinforced so that the actual maximum dynamic pressure (pulsation) amplitude is substantially greater than the induced pulsation. Thus at frequencies (pump speeds) corresponding to resonance, there would be considerably higher amplitude levels generated from the same amount of energy than for frequencies off resonance.

If the wave frequencies are such that the incident and reflected waves are additive, the pulsations are amplified. If no damping is present, the pressure amplitudes at the anti-nodes would, theoretically, go to infinity. Actual piping systems have acoustic damping as a result of:

- Viscous fluid action (intermolecular shearing).
- Transmission, i.e., lack of total reflection, at a line termination.
- Piping resistance, i.e., pipe roughness, restrictions, orifices.

Therefore, damping of acoustic modes may be accomplished by placement of resistance elements, such as an orifice, that will work most effectively at velocity maxima.

Length Resonances in Distributed Acoustic Systems. The concepts of acoustic waves, reflections, and resonance can be applied to describe some of the classical length resonances [13].

The length resonances of certain piping elements are described in terms of a full-wave length. The acoustic wave length is the distance required for a complete cycle of dynamic pressure reversal. The wave length is related to the driving frequency and the acoustic velocity or speed of sound:

$$\lambda = \frac{c}{f}$$

where λ = wave length, ft/cycle
c = acoustic velocity, ft/sec
f = driving frequency, Hz

Half-Wave Resonance (Open-Open and Closed-Closed)

The first three modes for an open-open pipe are shown in Figure 18-7. Resonances may also occur at integer multiples of the half-wave frequency. For a closed-closed pipe, the formula also applies since both elements have a standing wave that is one-half of a sine wave even though the peaks occur at different locations. The pressure mode shapes of the first three modes are also shown for the open-closed configuration. The length should be corrected for entrance and exit effects (add approximately 80% of the pipe inside diameter) to calculate the half-wave resonance of open-open configurations. The end correction factor becomes very important in short pipes.

Quarter-Wave Resonance (Open-Closed)

The first three modes for an open-closed pipe, commonly referred to as a "quarter-wave stub" are depicted in Figure 18-7. The stub has its resonant frequencies at odd integer multiples of the fundamental quarter-wave frequency. Examples of a quarter-wave stub include a bypass line with a closed valve or a test connection with a pressure gauge.

A quarter-wave resonance can cause erroneous measurements [13] when obtaining dynamic pressure data. A typical test connection, depicted in Figure 18-8, with a short nipple and valve connected to a main line is an acoustical quarter-wave stub. This length can tune up to pulsations in the main line and cause the needle on a pressure gauge to wobble or indicate severe pressure variations that do not actually exist in the main line. Similarly, the data from a dynamic pressure transducer can be misinterpreted.

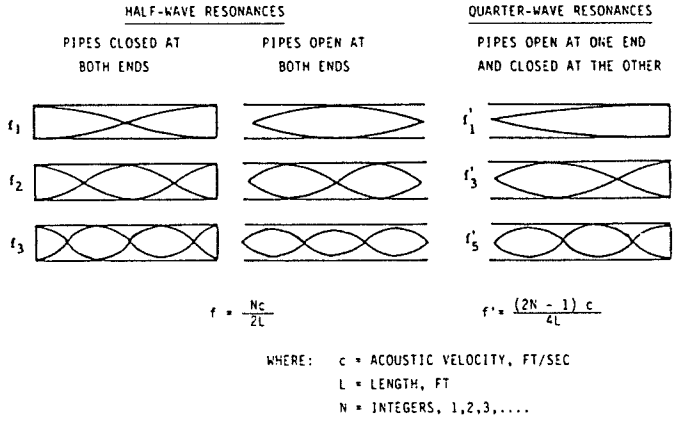

Figure 18-7. Acoustic resonances of piping elements.

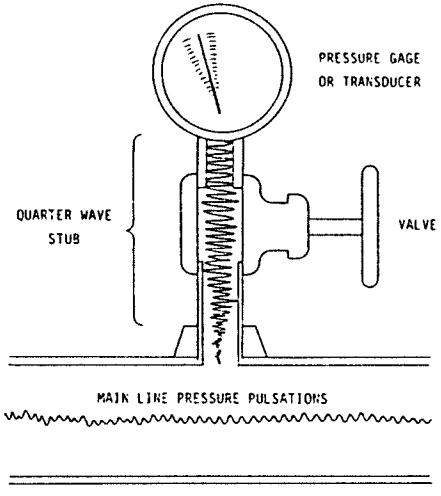

Figure 18-8. Erroneous pressure measurement caused by stub resonance.

For example, an installation where the speed of sound was 4500 ft/sec and the transducer was mounted one foot from the inside surface, the stub (quarter-wave) frequency would be 1125 Hz. A fictitious pressure pulsation component will be measured at this frequency and also at 3X, 5X, 7X, etc. The pulsation exists in the stub; however, it may not be present in the main pipe. If this stub frequency is close to the vane or blade passing frequency, the measured amplitude at the stub frequency will not be valid because it would be amplified by the acoustical resonance. The acoustical amplification factor can be as high as 200. To measure high-frequency pulsations, the transducer should be mounted flush to the inside surface of the pipe.

Measurements of peak-to-peak pulsations on an oscilloscope are often suspect. If the transducer signal frequency spectrum is analyzed and the quarter-wave resonance identified, then credible results can be obtained. An electronic filter may be used to eliminate the undesired frequency.

Coincidence of Driving Acoustic Frequencies and Length Resonances. The existence of quarter or half-wave natural frequencies alone does not constitute resonances. For resonance to occur, a dynamic pulse must be generated at a frequency equal to an acoustical natural frequency. The build-up in amplitude occurs because a reflected wave arrives at the proper time to reinforce the wave generated at the pump. The arrival of the reflected wave is dependent upon the path length of the piping elements. Therefore, the standing wave pattern amplitude is reinforced so that the actual maximum pulsating wave amplitude is substan-

tially greater than the induced level. Multiples of the resonant modes can be excited; however, the multiple wave length resonances generally decrease in severity at the higher multiples because more acoustic energy is required to drive the higher frequency modes.

The acoustic resonances of piping systems for constant-speed pumps can usually be adjusted to detune them from the pump operating speed and vane-passing frequencies and avoid pulsation amplification. However, if the pump is operated over a speed range, the frequency band of the excitations is widened, requiring more careful placement of acoustic resonances.

Actual piping systems are more complex than the simple quarter-wave and half-wave elements. A typical piping system with tees, flow control valves (restrictions) pipe size changes, vessels, etc., will have a complicated pattern of pressure pulse reflection patterns (standing waves). Some of the standing waves may be amplified and others, attenuated. Each of the standing waves will have a particular acoustic length pertaining to a pipe segment between two end conditions. Calculations of the acoustic resonances of a complex piping system require the use of computer codes to consider the acoustic interaction between the pump and its piping system.

Instabilities. Hydraulic instabilities [14] can be a result of the dynamic interaction of a centrifugal pump (particularly the head-flow characteristics) and the acoustic response of the piping system. A centrifugal pump operating at constant speed in a piping system may amplify or attenuate pressure disturbances that pass through the pump. The action of the pump in causing amplification or attenuation of this energy is quite complex, but basically is dependent upon:

- The head curve slope and operating point
- System flow damping (in the piping)
- The existence of strong reactive resonances in the piping, particularly if they coincide with vortex frequencies
- The location of the pump in the standing wave field (i.e., at a velocity maximum rather than a pressure maximum)
- The compressibility (bulk modulus) of the liquid

Pulsations can be amplified by the piping system and cause a variety of problems such as damage to pump internals, torsional reactions, cavitation, vibrations at elbows, valves, or other restrictions. The amplitude of the pulsation is dependent upon operating conditions such as speed, flow rate, and losses (pressure drop) as well as fluid properties and acoustic

natural frequencies. Consequently, pulsation amplitudes are usually affected by changes in the operating conditions or fluid composition.

Pulsations are commonly initiated by flow turbulence at changes in flow cross section, at restrictions (orifices, valves, etc.) or at the pump impeller. When the frequency of this turbulent energy excites one of the acoustic resonances of the piping system, and if the pump is situated near a velocity maximum in the resonant piping system, then high amplitude, self-sustaining pulsations can result. Pulsations can be minimized by moving the pump to a velocity minimum, but often a new pulsation frequency will be generated such that the pump is again situated near a velocity maximum for a higher mode oscillation. With proper care and detailed analysis of the relative strength of the various pulsation resonance modes of the piping, piping designs can be developed to avoid these strong resonances. Controlling piping stub lengths (i.e., in by-pass piping) so that their quarter-wave stub resonances are far removed from the Strouhal excitation frequencies, will also help in minimizing the potential for resonant pulsations.

This type of instability is more probable at low flows because acoustic damping that is generated by flow friction effects is greater at higher flow rates.

Design/Manufacturing

Dynamic response of the pump components to normal exciting forces within its operating frequency range can result in problems from excessive maintenance to catastrophic failure. Improper manufacture or assembly can cause unbalance resulting in damaging vibrations if the speed approaches natural frequencies of the rotor system. A rotordynamic audit [18] of the pump rotor design is crucial in avoiding speed-related vibrations.

The following section discusses the factors that are important in controlling the rotordynamic responses of a centrifugal pump.

Rotordynamic Analysis

A lateral critical speed is defined by API [7] as the speed at which a peak vibrational response occurs. At the critical speed, the rotor is more sensitive to unbalance than at any other speed. The critical speeds of a pump should be avoided to maintain acceptable vibration amplitudes. This section discusses the techniques involved in calculating the lateral critical speeds of centrifugal pumps.

Lateral Critical Speed Analysis

Pump rotordynamics are dependent on a greater number of design variables than are many other types of rotating equipment. Besides the journal bearing and shaft characteristics, the dynamic characteristics of the seals and the impeller-stationary lip interaction can have significant effects on the critical speed location, rotor unbalance sensitivity, and rotor stability [9, 19]. In this context, a seal is an element having a liquid film within a tight clearance. The liquid film has dynamic characteristics similar to a bearing. There are a variety of seal configurations including floating ring seals, grooved seals, and others. Several seal geometries will be discussed.

For modeling purposes, seals can be treated as bearings in the sense that direct and cross-coupled stiffness and damping properties can be calculated based on the seal's hydrostatic and hydrodynamic properties [20]. Seal clearances, geometry, pressure drop, fluid properties, inlet swirl, surface roughness, and shaft speed are all important in these calculations. The high pressure liquid being pumped also flows (or leaks) through the small annular spaces (clearances) separating the impellers under different pressures, such as wear rings and interstage bushings, and creates a hydrodynamic bearing effect that transforms the pump rotor from a two-bearing system to a multi-bearing system. The additional stiffness generated by the pumped liquid as it lubricates these internal bearings (seals, etc.) is referred to as the "Lomakin effect" [21].

The Lomakin stiffness effect minimizes the shaft deflections when the pump is running, and in some cases, the Lomakin effect can be of sufficient magnitude to prevent the critical speed of the rotor from ever being coincident with the synchronous speed. Since the pressure drop across seals increases approximately with the square of the pump speed, the seal stiffness also increases with the square of the speed.

The amount of support derived from the seals as bearings depends upon (a) the pressure differential, and therefore disappears completely when the pump is at rest, and (b) the clearance that increases significantly as the sealing surfaces wear. Consequently, contact between the rotor and stationary parts may take place each time the pump is started or stopped. In consideration of these facts, the rotordynamic analyses should include the effects of worn seals (loose clearances) as well as new seals (tight clearances).

Analytical techniques [22, 23, 24] have been developed whereby the seal geometry can be specified and the characteristics calculated for specific assumptions with regard to inlet swirl, groove design, etc. A series of grooved seal designs used in commercial pumps has been tested to verify the adequacy of the techniques.

A thorough lateral critical speed analysis is essential for developing a reliable, trouble-free pump system. The design audit [18] should include the following calculations:

- Critical speed map
- Undamped natural frequencies and mode shapes
- Bearing stiffness and damping properties
- Seal stiffness and damping properties
- Rotor response to unbalance
- Pedestal and foundation effects on response
- Rotor stability

The first step in performing a lateral critical speed analysis is to model the shaft with sufficient detail and number of masses to accurately simulate the rotor responses through its speed range. An accurate shaft drawing giving the dimensions, weights, and centers of gravity of all added masses is needed to develop the model. Generally, each significant shaft diameter change is represented by one or more stations. A station is generally located at each added mass or inertia, at each bearing and seal location, and at each potential unbalance location. A typical rotor shaft drawing and the computer model is given in Figure 18-9.

Rotating elements such as impellers are modeled as added masses and inertias at the appropriate locations on the shaft. The polar and transverse mass moments of inertia are included in the analyses to simulate the gyroscopic effects on the rotor. The gyroscopic effects are particularly significant on overhung rotors where the impeller produces a restoring moment when whirling in a deflected position.

Couplings are simulated as concentrated added weights and inertias. Normally half the coupling weight is placed at the center of gravity of the half coupling. When necessary, the entire train, including the driver and driven equipment, can be modeled by utilizing programs that can simulate the shear loading and moment transfer across the coupling. Once the shaft model is completed, the critical speed map can be calculated.

Critical Speed Map. The critical speed map is a logarithmic plot of the undamped lateral critical speeds versus the combined support stiffness, consisting of the bearing and support structure as springs in series. The critical speed map provides the information needed to understand the basic response behavior of rotors; therefore, it is important to understand how the map is developed [25].

For large values of support stiffness, the rotor critical speeds are called the rigid bearing critical speeds. If the bearing stiffness is infinity, the vibrations are zero at the bearings, and the first natural frequency for

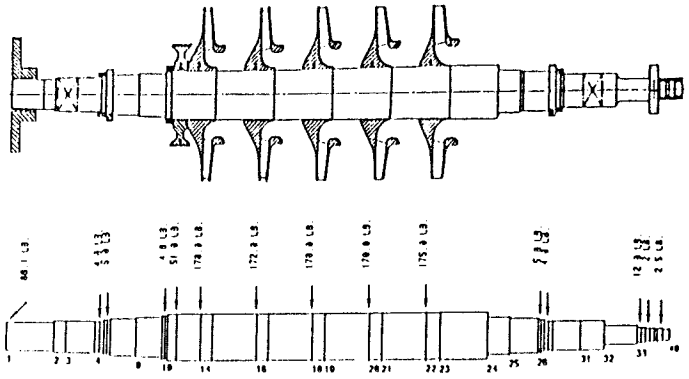

Figure 18-9. Typical shaft drawing and computer model.

shafts that do not have overhung impellers is analogous to a simply supported beam.

A critical speed map, normalized to the first rigid bearing critical speed is given in Figure 18-10 to illustrate the ratios of the various criticals for low and high support stiffness values and to illustrate the mode shapes that the rotor will have at different bearing and support stiffness values. For the rigid bearing critical speeds, the mode shape for the first mode would be a half-sine wave (one loop), the second critical speed would be a two-loop mode and would occur at a frequency of four times the first mode critical, the third critical speed would be a three-loop mode and would be nine times the first critical, etc. For most rotors, the bearing stiffnesses are less than rigid and the second critical will be less than four times (typically two–three times) the first critical.

For low values of support stiffness (shaft stiffness is large compared to support stiffness), the first critical speed is a function of the total rotor weight and the sum of the two support spring stiffnesses. For an ideal long slender beam, the second mode is similar to the rocking of a shaft on two springs and is equal to 1.73 times the first critical speed. Since both the first and second modes are a function of the support stiffness, the slope of the frequency lines for the first and second critical speeds versus support stiffness is proportional to the square root of the stiffness for low values of support stiffness compared to the shaft stiffness.

For a support stiffness of zero, the third and fourth modes would be analogous to the first and second free-free modes of a beam. For an ideal uniform beam, the ratio of the frequencies for these modes compared to the first critical speed for rigid bearings is 2.27 and 6.25.

To aid in the discussion, an example of the critical speed analysis [9] of an eight-stage pump will be presented. The critical speed map for the

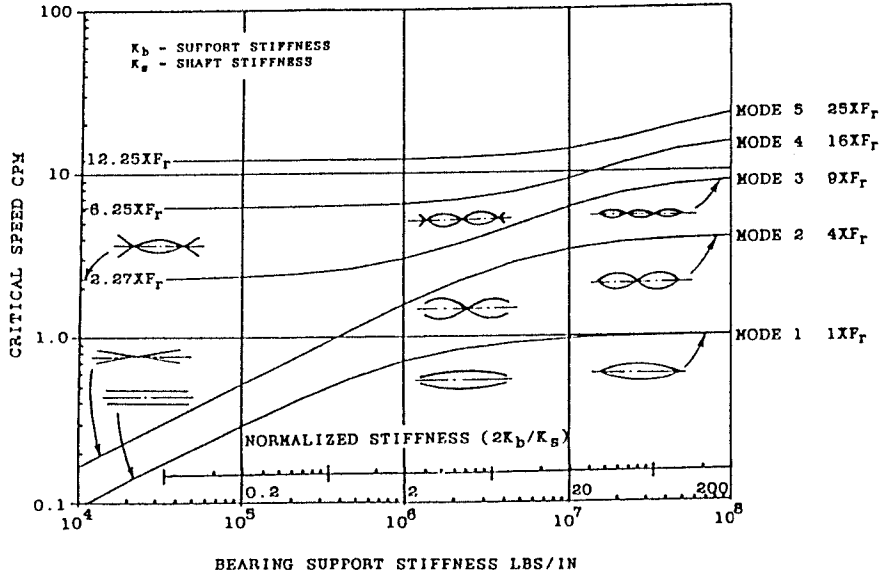

Figure 18-10. Normalized critical speed map.

"dry rotor" model (without the hydrodynamic effect of the seals) is shown in Figure 18-11. The first four undamped lateral critical speeds are plotted versus bearing support stiffness. Horizontal and vertical journal bearing stiffness curves (Kxx and Kyy) for both minimum and maximum assembled clearances are plotted to define the range of critical speeds. Intersections between the bearing stiffness curves and the mode curves represent undamped critical speeds (circled in Figure 18-11). Note that the "Mode 1" curve is fairly flat in the region where the intersections occur. The first two lateral mode shapes were calculated for a nominal bearing stiffness of 500,000 lb/in. and are shown in Figures 18-12 and 18-13. The dry rotor undamped natural frequencies as predicted by the critical speed map for the first, second, and third modes were 1710, 6650, and 8830 cpm, respectively.

Bearing Stiffness and Damping. The dynamic stiffness and damping coefficients of bearings [26] can be adequately simulated using eight linear coefficients (Kxx, Kyy, Kxy, Kyx, Cxx, Cyy, Cxy, Cyx) as shown in Figure 18-14. This information along with the lubricant minimum film thickness, flow, power loss, and temperature rise at operating conditions is needed to evaluate the bearing design. The bearing stiffness and damping coefficients are calculated as functions of the bearing type, length,

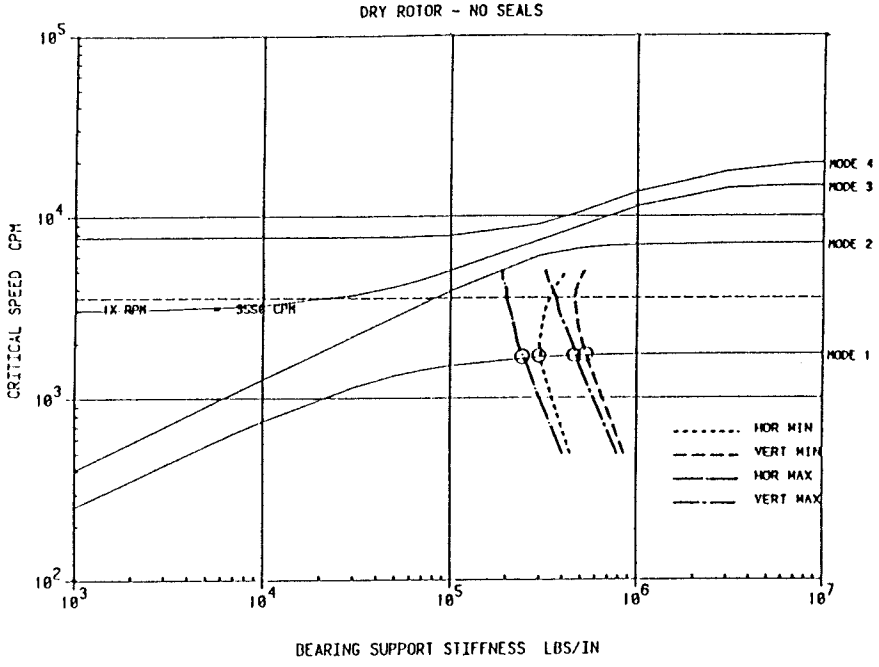

Figure 18-11. Eight-stage pump critical speed map—no seals.

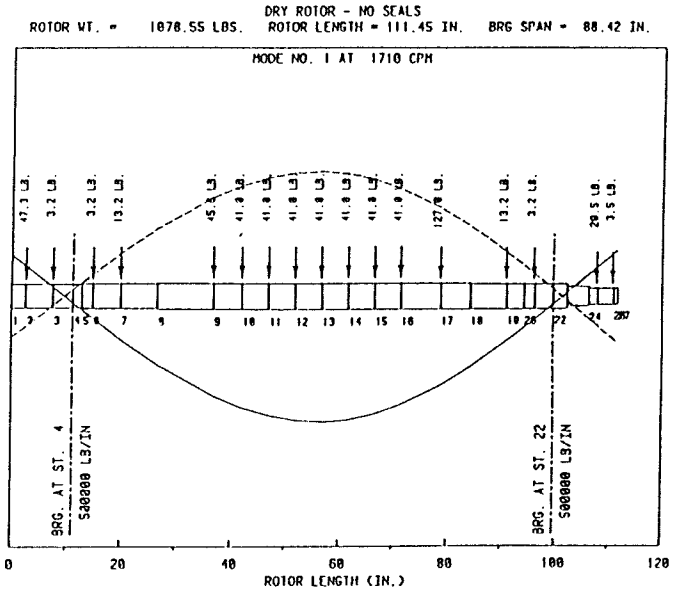

Figure 18-12. Eight-stage pump—first mode response—no seals.

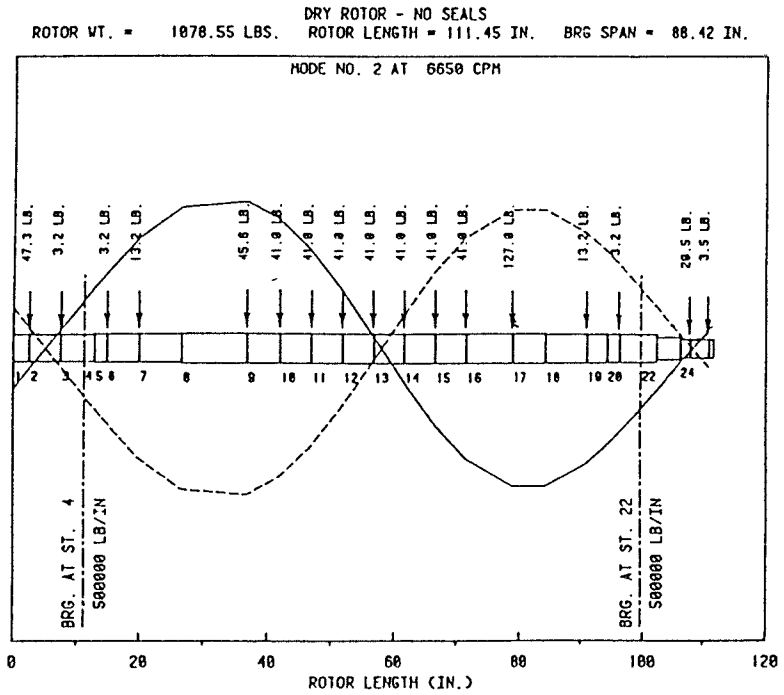

Figure 18-13. Eight-stage pump—second mode response—no seals.

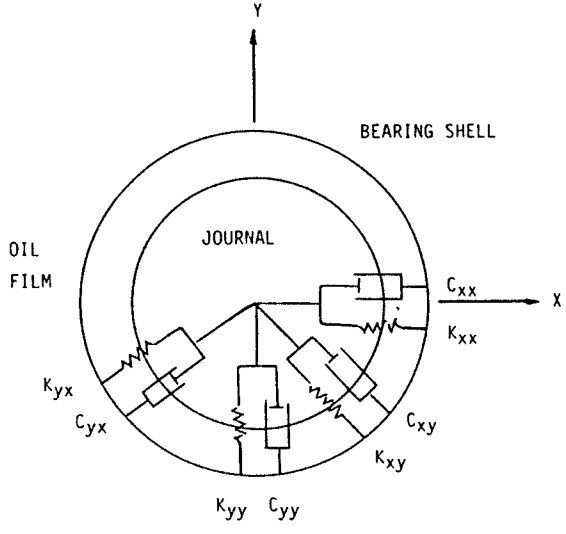

Figure 18-14. Hydrodynamic bearing stiffness and damping coefficients.

diameter, viscosity, load, speed, clearance, and the Sommerfeld number that is defined as:

$$S = \frac{\mu NDL}{W}\left(\frac{R}{C}\right)^2$$

μ = lubricant viscosity, lb-sec/in.
N = rotor speed, rev/sec
D = bearing diameter, in.
L = bearing length, in.
R = bearing radius, in.
W = bearing load, lbs
C = radial machined clearance, in.

The normal procedure in a design audit would be to calculate the bearing characteristics for the range of expected clearances, preload, and oil temperatures. The maximum clearance, minimum preload, and highest oil temperature usually define the minimum stiffness. The other extreme is obtained from the minimum clearance, maximum preload, and the coldest oil temperature. This will typically define the range of expected stiffness and damping coefficients for the bearings.

Preload is a configuration of the bearing clearances to promote a converging wedge of oil that increases the oil pressure and consequently the bearing stiffnesses. A preloaded bearing has its radius of curvature greater than the shaft radius plus the clearance.

Seal Effects

The critical speed map for a eight-stage pump, including the effects of seal and bearing stiffness, is given in Figure 18-15. Even though the bearings and seals add considerable cross-coupling and damping, it is still desirable to generate an undamped critical speed map to establish the range of the undamped (dry) critical speeds.

Adequate experimental data exists that documents that the analytical procedures used for simulating rotor response and stability for compressors and turbines can accurately predict critical speeds and potential instabilities from the design information. This is not true for pumps, especially for pumps that use grooved seals, labyrinth seals, or screw type seals with several leads. The accurate prediction of the stiffness and damping properties of seals for different geometries and operating conditions is a subject of on-going research [22, 27, 28]. The basic theories presented by Black [29] have been modified to account for finite length

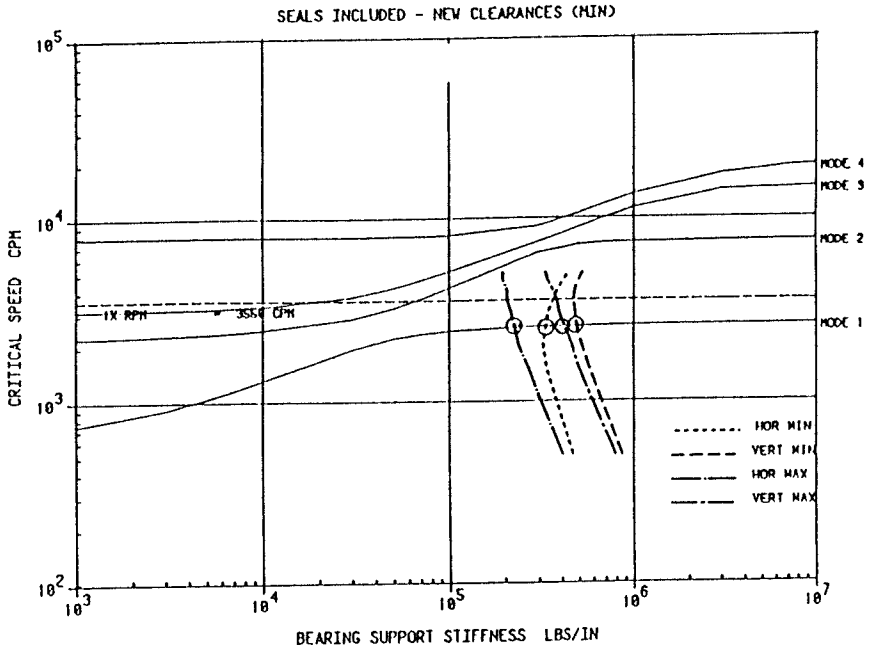

Figure 18-15. Eight-stage pump critical speed map—seals included.

seals, inlet swirl, groove, and other important parameters. However, a universally accepted procedure to accurately predict seal properties is not available for all the seal types that are in use today. If the seal effects are not correctly modeled, calculated critical speeds can be significantly different from actual critical speeds.

The forces in annular pressure seals can have a significant effect on the vibration characteristics of a pump rotor. The hydrodynamic and hydrostatic forces involved can significantly affect unbalanced response characteristics. The fluid film interaction with the shaft and the pressure drop across the seal give rise to a load capacity and a set of dynamic stiffness and damping coefficients similar to those used to represent the oil film in journal bearings.

Unlike hydrodynamic bearings, seals develop significant direct stiffness in the centered, zero-eccentricity position due to the distribution of the axial pressure drop between the inlet losses and an axial pressure gradient due to friction losses. The cross-coupled stiffnesses arise due to fluid rotation (swirl) within the seal. As a fluid element proceeds axially along an annular seal, shear forces at the rotor accelerate or decelerate the fluid tangentially until an asymptotic value is reached. For a seal with the same directionally homogeneous surface-roughness treatment on the

rotor and the housing, the average asymptotic tangential velocity is $R\omega/2$, where R is the seal radius and ω is the rotor running speed. The cross-coupled stiffness coefficient (K) acts in opposition to the direct damping coefficient (C) to destabilize rotors. Hence, steps that can be taken to reduce the net fluid rotation within a seal will improve rotor stability [30] by reducing K.

Childs has defined the dynamic seal coefficients for plain short seals directly from Hirs' lubrication equations [27] and has included the influence of fluid inertia terms and inlet swirl. His assumptions are less restrictive than previous derivations. The derived coefficients are in reasonable agreement with prior results of Black and Jenssen.

Childs [28] has extended the analysis to include finite-length seals. This analysis includes variable inlet swirl conditions (different from $R\omega/2$) and considers variations in the axial and circumferential Reynolds numbers due to changes in clearances.

A combined analytical-computational method has also been developed by Childs [28] to calculate the transient pressure field and dynamic coefficients for interstage and neck ring seals of multistage centrifugal pumps. The solution procedure applies to constant-clearance or convergent-tapered geometries that may have different surface-roughness treatments of the stator or rotor seal elements. The method has been applied to the calculation of "damper" seals as described by von Pragenau [31] and several roughened stator designs, such as knurled-indentation, diamond-grid post pattern, and round-hole pattern, have been tested. These procedures can be used to calculate serrated or grooved seals of various geometries.

Critical Speed Map—Considering Seals. The seal configurations at the balance piston, neck ring, and interstage bushings of the eight-stage pump are shown in Figure 18-16. The critical speed map (Figure 18-15) includes the support stiffnesses of the neck ring seals and interstage bushings combined at each impeller. The seal stiffness and damping coefficients are listed in Table 18-2 for nominal clearances. Note that a negative principal stiffness (K) value is predicted for the balance piston.

For this analysis the pump rotor was analyzed as if it had 11 bearings consisting of two tilted-pad bearings, the balance piston, and eight seals located at the impellers. For the purposes of developing the critical speed map, the seal stiffness values were held constant at their maximum levels (minimum clearances) that represent new seals.

The lateral mode shape of the first critical speed including these seal effects is shown in Figure 18-17. A bearing stiffness value of 500,000 lb/in. was again used for the mode shape calculations. Comparing Figure 18-17 with Figure 18-12, it is seen that the seals increase the frequency of

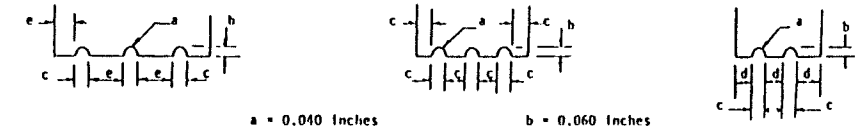

BALANCE PISTON	NECK RING	INTERSTAGE BUSHING
32 LANDS - 0.24"	4 LANDS - 0.12"	3 LANDS - 0.16"
31 GROOVES - 0.12"	3 GROOVES - 0.12"	2 GROOVES - 0.12"
DIAMETER - 8.858"	DIAMETER - 8.858"	DIAMETER - 6.496"
DIAMETRICAL CL - 0.020"	DIAM. CL. - 0.020"	DIAM. CL. - 0.018"
PRESS. DROP - 2800 PSI	PRESS. DROP - 340 PSI	PRESS. DROP - 4 PSI

FLUID PROPERTIES: WATER @ 150° F; DENSITY - 0.0354 LB/IN^3
VISCOSITY - 6.28×10^{-8} LB-SEC/IN

Figure 18-16. Eight-stage pump seal geometries and fluid properties.

Table 18-2
Summary of Seal Coefficients

	Stiffness		Damping	
Seal Type	Principal K-lb/in	Cross-Coupled K-lb/in	Principal C-lb sec/in	Cross-Coupled C-lb sec/in
Neck-Ring	13,400	4900	23	0
Int-Stg Bush	-8	370	3	0
Balance Piston	-271,000	627,000	25,000	3000

the first mode without altering the mode shape significantly. For an assumed bearing stiffness of 500,000 lb/in., the first, second, and third critical speeds from Figure 18-15 are 2570, 7120, and 8830 cpm.

Evaluation of Critical Speed Calculations. To summarize, in the evaluation of the adequacy of the rotor from the critical speed map and the mode shapes, the following items should be examined [18]:

- *The proximity of the critical speed to running speed or speed range.* The undamped lateral critical speeds should not coincide with the running speed. Various codes [7] address the allowable margin between lateral critical speeds and exciting frequencies. To determine if the actual critical speed will cause excessive vibrations, a rotor response to unbalance analysis should be performed.

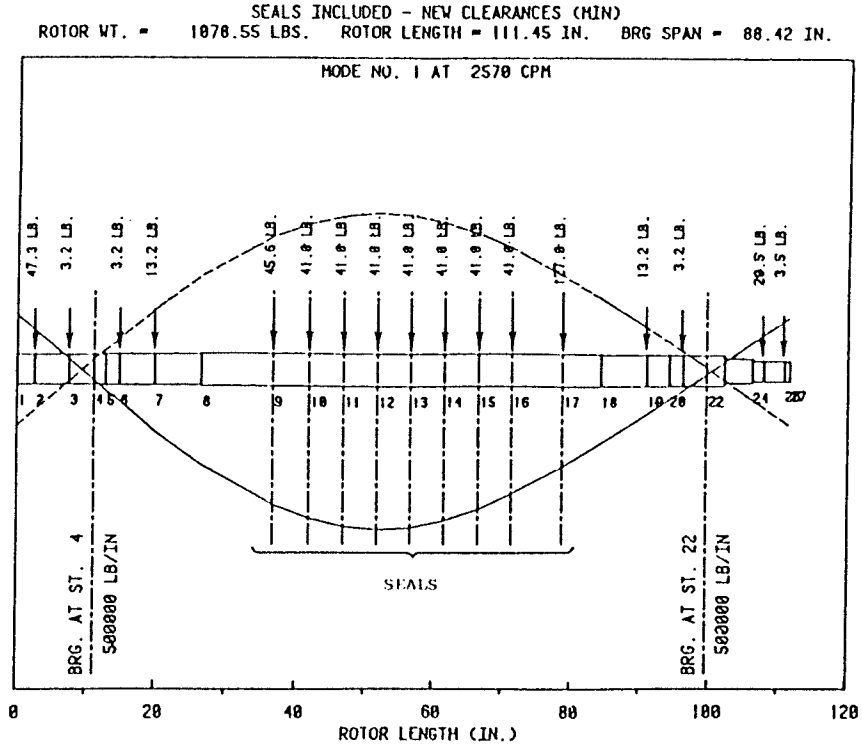

Figure 18-17. Eight-stage pump—first mode response—seals included.

- *The location of the critical speed relative to the support stiffness.* If the critical speed is near the rigid bearing criticals (flexible shaft region), increasing the bearing stiffness will not increase the critical speed because the weaker spring controls the resonant frequency. Vibration amplitudes may be low at the bearings (first mode), and therefore, low damping will be available. This can contribute to rotordynamic instabilities that will be discussed later. If the critical speeds are in the area of low support stiffness (stiff shaft region), the critical speeds are strongly dependent upon the bearing stiffness and damping characteristics and the critical speeds will be dependent upon bearing clearance. Bearing wear could be a significant problem.
- *The mode shape of the critical speed.* The mode shapes are used to assess the response of the rotor to potential unbalances. For example, a rotor that has a conical whirl mode (second critical) would be sensitive to coupling unbalance, but not strongly influenced by midspan unbalance.

Response To Unbalance

The location of a pump critical speed is defined by its response to unbalance. It is important to recognize the difference between critical speeds excited by unbalance and damped eigenvalues that are frequently also called critical speeds [32]. Generally, the effect of damping is to raise the frequency of the critical speed response due to unbalance; however, the effect of damping on the damped eigen values is to lower the frequency. The damped eigenvalues are primarily used for evaluating the stability of the rotor system. For compressors and turbines with tilting pad bearings, the damped eigenvalues are usually comparable to the unbalanced response criticals. However, in a pump with a large number of seals, the added damping to the system can be considerable, resulting in large differences in the unbalanced response critical speeds and the damped eigenvalues.

Rotor unbalance response calculations are the key analysis in the design stage for determining if a pump rotor will be acceptable from a dynamics standpoint. An accurate prediction of rotor unbalanced response is difficult for centrifugal pumps because of the sensitivity to bearing and seal clearances that may be at the tight or loose end of the tolerance range.

Computer programs are available that can calculate the elliptical shaft orbit at any location along the length of a rotor for various types of bearings, pedestal stiffnesses, pedestal masses, seals, labyrinths, unbalance combinations, etc. These programs can be used to determine the response of the installed rotor to unbalance and accurately predict the critical speeds over the entire range of variables. The actual critical speed locations as determined from response peaks caused by unbalance are strongly influenced by the following factors [33]:

- bearing direct stiffness and damping values
- bearing cross-coupled stiffness and damping values
- location of the unbalance
- location of measurement point
- bearing support flexibility

The normal unbalance used in the analysis would produce a force equal to 10% of the rotor weight at operating speed. Usually the rotor response to unbalance calculations are independently made for midspan unbal-

ance, coupling unbalance, and moment unbalance. An unbalance equal to a force of 5% of the rotor weight is usually applied at the coupling to excite the rotor. For moment unbalance, an unbalance equal to 5% of the rotor weight is used at the coupling and another equal unbalance is used out-of-phase on the impeller furthest from the coupling.

The unbalance response of a pump should be analyzed for several cases to bracket the expected range of critical speeds. The first analysis should include minimum seal and bearing clearances that represent the maximum expected support stiffness and therefore, the highest critical speed. The second analysis should consider the maximum bearing clearances and seal clearances of twice the design clearance to simulate the pump condition after long periods of service. The third analysis should simulate the worn condition with no seal effects and maximum bearing clearances that represent the overall minimum expected support stiffness for the rotor (lowest critical speed).

The unbalanced response of the eight-stage pump with maximum bearing clearances and no seals is shown in Figure 18-18. The peak response at 1700 rpm was the minimum calculated critical speed. The unbalance was applied at the rotor midspan to excite the first mode. The response for the intermediate analysis (worn seals) is plotted in Figure 18-19. The worn seals increased the predicted response peak to approximately 1800 cpm. With minimum clearances at the bearings and seals, the response was lower and the frequency increased to 2200 cpm, as shown in Figure 18-20 (note scale changes).

Shop acceptance test data was available for the eight-stage pump which was analyzed. The calculated unbalanced response is compared with the measured vibration data from the test stand in Figure 18-21. For these calculations, maximum bearing clearance and the design values of seal clearance were used. Based on these results, Childs' finite length method [28] provides favorable results compared with measured data. The "shape" of the response curve using Childs' seal values compares closely with the measured results, indicating that the damping contribution of the seals is of the right magnitude.

The anticipated range of rotor response should be calculated with the range of bearing values and various combinations of unbalance. This is important because it is not possible in the design stage to know the exact installed configuration with regard to bearings (clearance, preload) and balance (location of unbalance). Usually a mechanical test will be limited to one configuration (clearance, preload, unbalance) that may not show any problem. Changes introduced later by spare parts during maintenance turnarounds may change sensitive dimensions that may result in a higher response. For this reason, the vibration characteristics of some satisfactorily operating machines may change after an overhaul.

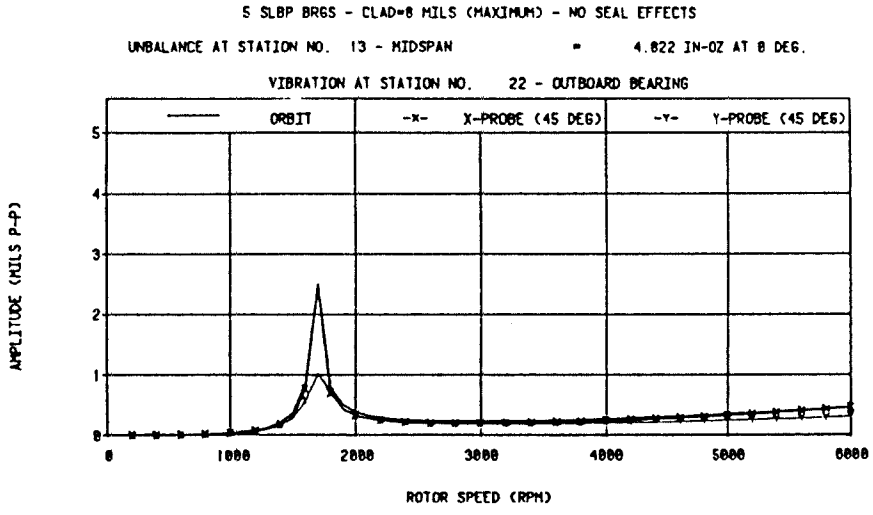

Figure 18-18. Unbalance response at outboard bearing with API unbalance at midspan—no seals.

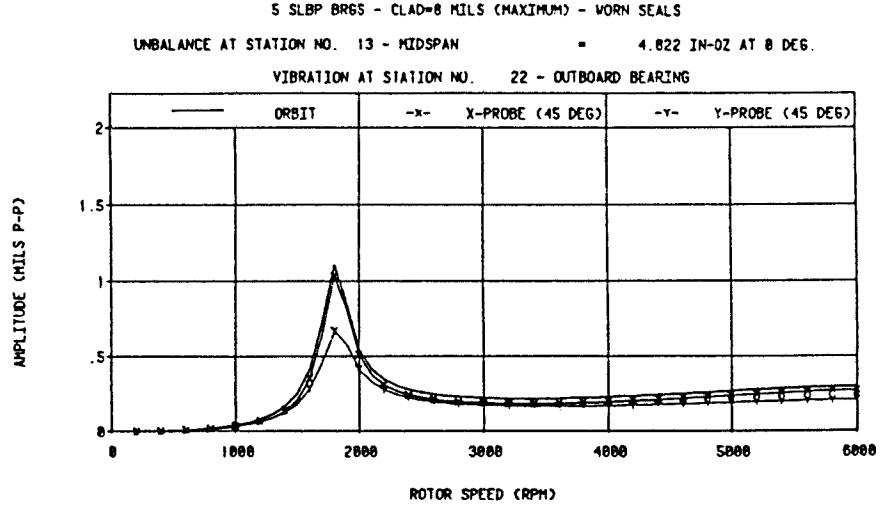

Figure 18-19. Unbalance response at outboard bearing with API unbalance at midspan—maximum clearance seals.

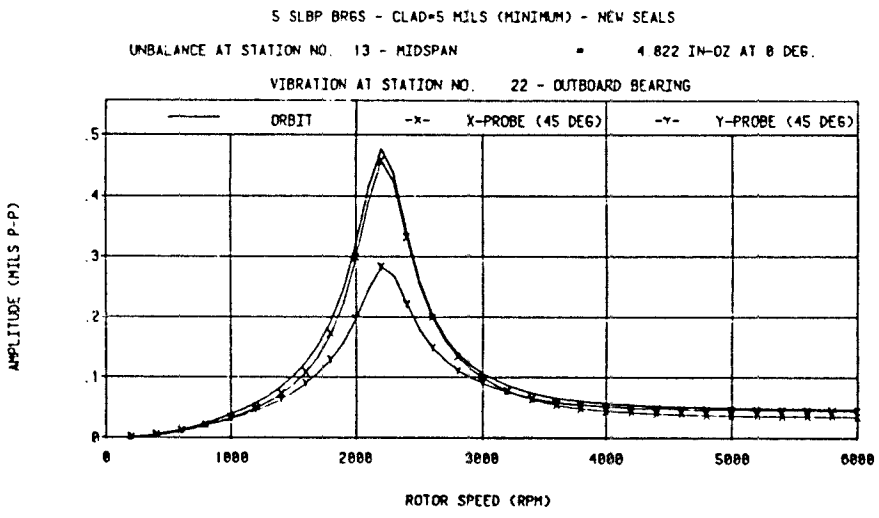

Figure 18-20. Unbalance response at outboard bearing with API unbalance at midspan—minimum clearance seals.

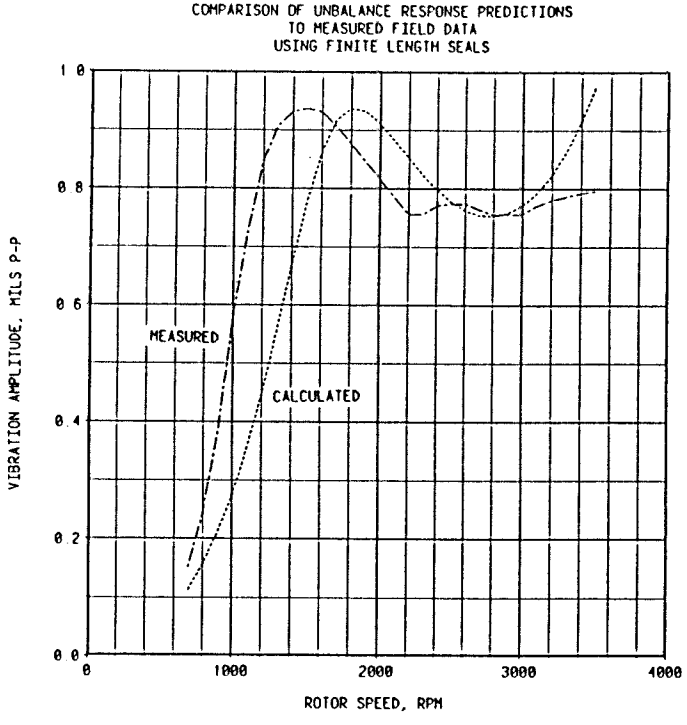

Figure 18-21. Comparison of calculated and measured response with seals.

Acceptable Unbalance Levels

Various engineering organizations have set forth criteria for allowable residual unbalance. The Acoustical Society of America defines balance quality grades for various types of rotors as described in Table 18-3. Pumps may have a range of balance quality grade from G2.5 to G6.3 depending upon size. The ASA Standard 2-1975 defines maximum residual unbalance [34] that is dependent upon speed as shown in Figure 18-22. For example, a 3,600 rpm pump with a rotor weight of 1,000 lbs for balance grade G2.5 would have an allowable residual unbalance of 4.5 in.-oz.

The revised API-610 (seventh edition, 1989) specifies an allowable residual unbalance for centrifugal pumps. The maximum allowable residual unbalance per plane (journal) may be calculated by the following formula:

$$U_b = \frac{4W}{N_{mc}}$$

where U_b = allowable unbalance, inch-ounces
W = journal static weight load, lbs
N_{mc} = maximum continuous speed, rpm

The total allowable unbalance (two planes near the journals) for a 3,600 rpm pump with a 1,000 lb rotor would be 1.1 in.-oz. This calculated residual unbalance from the current edition of the API code is significantly less than the allowable unbalance from earlier editions of the API codes for speeds less than 10,000 rpm. The previous edition of API-610 simply specified dynamic balance for all major rotating components with no specific value for an allowable unbalance. The various balance criteria are compared in Figure 18-23 for a 1,000 lb rotor.

Allowable Vibration Criteria

It is difficult to define the absolute maximum vibration level that can be tolerated without damage to the rotor. Some allowable vibration criteria are based on bearing housing vibrations. With rolling element bearings, the ratio of shaft vibrations to case vibrations is close to unity. The API-610 [7] specifies that the unfiltered vibration measured on the bearing housing should not exceed a velocity of 0.30 ips (inches per second) nor exceed a displacement of 2.5 mils peak-peak at rated speed and capacity $\pm 10\%$.

Table 18-3
Balance Quality Grades for Various Groups of Representative Rigid Rotors

Balance quality grades G	$s\omega$[a,b] (mm/sec)	Rotor types—General examples
G 4 000	4 000	Crankshaft-drives[c] of rigidly mounted slow marine diesel engines with uneven number of cylinders.[d]
G 1 600	1 600	Crankshaft-drives of rigidly mounted large two-cycle engines.
G 630	630	Crankshaft-drives of rigidly mounted large four-cycle engines. Crankshaft-drives of elastically mounted marine diesel engines.
G 250	250	Crankshaft-drives of rigidly mounted fast four-cylinder diesel engines.[d]
G 100	100	Crankshaft-drives of fast diesel engines with six or more cylinders.[d] Complete engines (gasoline or diesel) for cars, trucks, and locomotives.[e]
G 40	40	Car wheels, wheel rims, wheel sets, drive shafts Crankshaft-drives of elastically mounted fast four-cycle engines (gasoline or diesel) with six or more cylinders.[d] Crankshaft-drives for engines of cars, trucks, and locomotives.
G 16	16	Drive shafts (propeller shafts, cardan shafts) with special requirements. Parts of crushing machinery. Parts of agricultural machinery. Individual components of engines (gasoline or diesel) for cars, trucks, and locomotives. Crankshaft-drives of engines with six or more cylinders under special requirements. Slurry or dredge pump impeller.
G 6.3	6.3	Parts or process plant machines. Marine main turbine gears (merchant service). Centrifuge drums. Fans. Assembled aircraft gas turbine rotors. Fly wheels. Pump impellers. Machine-tool and general machinery parts. Normal electrical armatures. Individual components of engines under special requirements.
G 2.5	2.5	Gas and steam turbines, including marine main turbines (merchant service). Rigid turbo-generator rotors. Rotors. Turbo-compressors. Machine-tool drives. Medium and large electrical armatures with special requirements. Small electrical armatures. Turbine-driven pumps.
G 1	1	Tape recorder and phonograph (gramophone) drives. Grinding-machine drives. Small electrical armatures with special requirements.
G 0.4	0.4	Spindles, disks, and armatures of precision grinders. Gyroscopes.

[a] *$\omega = 2\pi n/60 \approx n/10$, if n is measured in revolutions per minute and ω in radians per second.*
[b] *In general, for rigid rotors with two correction planes, one-half of the recommended residual unbalance is to be taken for each plane, these values apply usually for any two arbitrarily chosen planes, but the state of unbalance may be improved upon at the bearings. (See Ses. 3.2 and 3.4.) For disk-shaped rotors the full recommended value holds for one plane. (See Sec. 3.)*
[c] *A crankshaft-drive is an assembly which includes the crankshaft, a flywheel, clutch, pulley, vibration damper, rotating portion of connecting rod, etc. (See Sec. 3.5.)*
[d] *For purposes of this Standard, slow diesel engines are those with a piston velocity of less than 9 m/sec; fast diesel engines are those with a piston velocity of greater than 9 m/sec.*
[e] *In complete engines, the rotor mass comprises the sum of all masses belonging to the crankshaft-drive described in Note c above.*

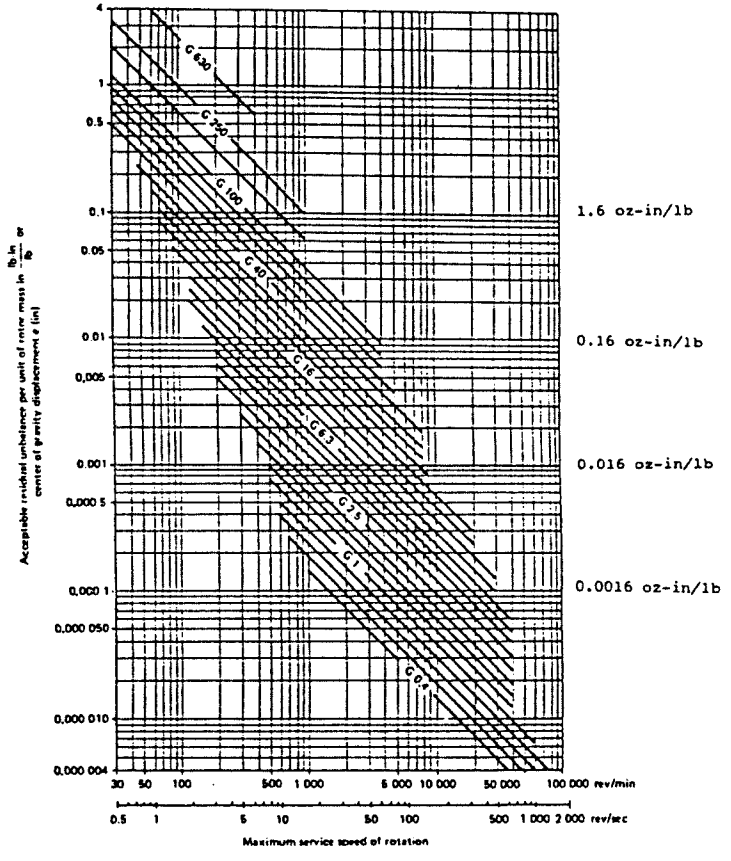

Figure 18-22. Allowable residual unbalance for industrial machinery ASA Standard 2-1975 [34].

However, with oil film bearings, the clearance between the shaft and bearings and the damping of the oil reduces the vibrational force transmitted to the case. For rotors with oil film bearings, shaft vibrations are a better indicator of unbalance conditions. The API-610 allowable vibrations for pumps with sleeve bearings (oil film) are based on shaft vibration measured at rated speed and capacity. The API-610 specifies the allowable unfiltered vibration shall not exceed a velocity of 0.40 ips nor exceed a displacement of 2.0 mils peak-peak including shaft runout.

For critical installations, vibration monitoring equipment should include non-contacting proximity probes (vertical and horizontal) at each

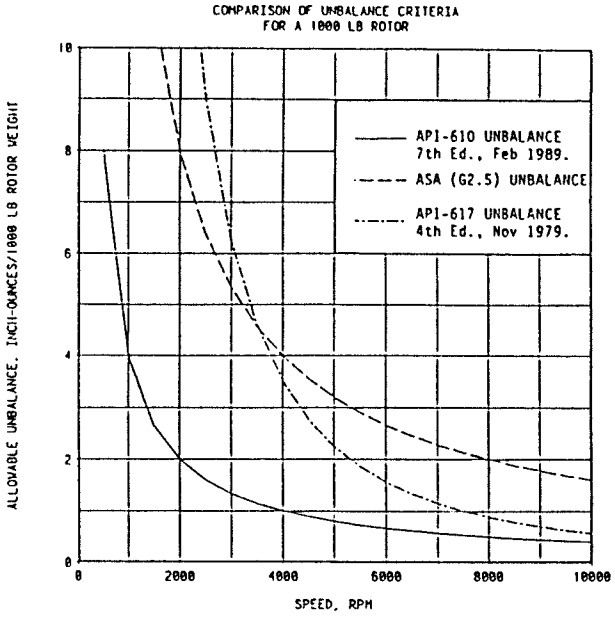

Figure 18-23. Comparison of residual unbalance criterion.

bearing. These vibrations should be continuously monitored with provision made for automatic alarm and shutdown capabilities to protect the installation from damage.

For oil film bearings, the following guidelines for defining maximum acceptable vibration levels are sometimes used when code allowables do not apply. If the vibrations are less than one-fourth of the diametrical bearing clearance, then the vibrations may be considered acceptable. Vibration amplitudes (A, peak-to-peak) greater than one-half the diametrical clearance (C_d) are unacceptable, and steps should be taken to reduce them.

$$A < \frac{C_d}{4} \text{ acceptable}$$

$$\frac{C_d}{4} < A < \frac{C_d}{2} \text{ marginal}$$

$$A > \frac{C_d}{2} \text{ unacceptable}$$

As with most experience-based criteria, these allowable amplitudes are based upon the synchronous vibration component only. Many manufacturers however, still assess acceptable vibrations on their equipment by case or bearing housing vibrations. In plant preventative maintenance programs, hand-held velocity pickups are commonly used to monitor vibrations.

Rotor Stability Analyses

Stability continues to be of major concern for rotors with hydrodynamic bearings, especially for high pressure pumps [36, 37]. In high performance pumps with vaned diffusers, large hydraulic forces can be exerted on the rotor at partial loads. The close internal clearances of pressure retaining seals create hybrid bearings that can produce a destabilizing effect.

Rotor instability occurs when the rotor destabilizing forces are greater than the rotor stabilizing forces. The destabilizing forces can be caused by: the bearings, seals, rotor unbalance, friction in shrink fits, or by loading effects such as inlet flow mismatching the impeller vane angle, turbulence at impeller tips, pressure pulsations, and acoustical resonances.

Instabilities in rotors can cause high vibrations with several different characteristics. They generally can be classified as bearing-related and self-excited. Oil whirl and half-speed whirl are bearing-related instabilities and are caused by the cross-coupling from the bearing stiffness and damping in fixed geometry bearings. Half-speed whirl will result in rotor vibrations at approximately one-half of the running speed frequency. Oil whirl describes a special type of subsynchronous vibration that tracks approximately half-speed up to the point where the speed is two times the first critical. As the speed increases, the subsynchronous vibration will remain near the first critical speed. These types of instabilities can generally be solved by changing the bearing design to a pressure dam, elliptical, offset-half bearing, or a tilting pad bearing.

Self-excited instability vibrations can occur on any rotor, including those with tilted pad bearings. The vibrations will usually occur near the rotor first critical speed or may track running speed at some fractional speed. These types of instability vibrations are sometimes called self-excited vibrations because the motion of the rotor creates the forcing mechanism that causes the instability.

The predominant method used in performing a stability analysis [38] is to calculate the damped (complex) eigenvalues and logarithmic decrement (log dec) of the rotor system including the bearings and seals. The log dec is a measure of the damping capability of the system to reduce

vibrations by absorbing some of the vibrational energy. A positive log dec indicates that a rotor system can damp the vibrations and remain stable, whereas a negative log dec indicates that the vibration may actually increase and become unstable. Experience has shown that due to uncertainties in the calculations, the calculated log dec should be greater than + 0.3 to ensure stability. The damped eigenvalue and log dec are sometimes plotted in a synchronous stability map. The frequency of damped eigenvalues is generally near the shaft critical speeds; however, in some heavily damped rotors it can be significantly different from the unbalanced response.

Rotor stability programs are available that can model the rotor stability for most of the destabilizing mechanisms; however, some of the mechanisms that influence it are not clearly understood. It has been well documented that increased horsepower, speed, discharge pressure, and density can cause a decrease in the rotor stability. Many rotors that are stable at low speed and low pressure become unstable at higher values. To predict the stability of a rotor at the design operating conditions, the rotor system is modeled and the log dec is calculated as a function of aerodynamic loading.

Torsional Critical Speed Analysis

All rotating shaft systems have torsional vibrations to some degree. Operation on a torsional natural frequency can cause shaft failures without noticeable noise or an obvious increase in the lateral vibrations. In geared systems, however, gear noise may occur that can be a warning of large torsional oscillations. Therefore, it is important to ensure that all torsional natural frequencies are sufficiently removed from excitation frequencies.

A torsional analysis should include the following:

- Calculation of the torsional natural frequencies and associated mode shapes.
- Development of an interference diagram that shows the torsional natural frequencies and the excitation components as a function of speed.
- Calculation of the coupling torques to ensure that the coupling can handle the dynamic loads.
- Calculation of shaft stresses, even if allowable margins are satisfied.
- Calculation of transient torsional stresses [39] and allowable number of starts for synchronous motor drives.

Torsional natural frequencies are a function of the torsional mass inertia and the torsional stiffness between the masses. The natural frequencies and mode shapes are generally calculated by the Holzer method or by eigenvalue-eigenvector procedures [40]. Either of the methods can give accurate results. A good design practice would be to locate the torsional natural frequencies a minimum margin of 10% from all potential excitation frequencies.

An example of the mass-elastic diagram of a torsional system of a 3,600 rpm motor-driven, six-stage pipeline pump is given in Figure 18-24. The natural frequencies and mode shapes associated with the first four natural frequencies are given in Figure 18-25. The mode shapes can be used to determine the most influential springs and masses in the system. This information is important if a resonance is found near the operating speed and system changes must be made to detune the frequencies.

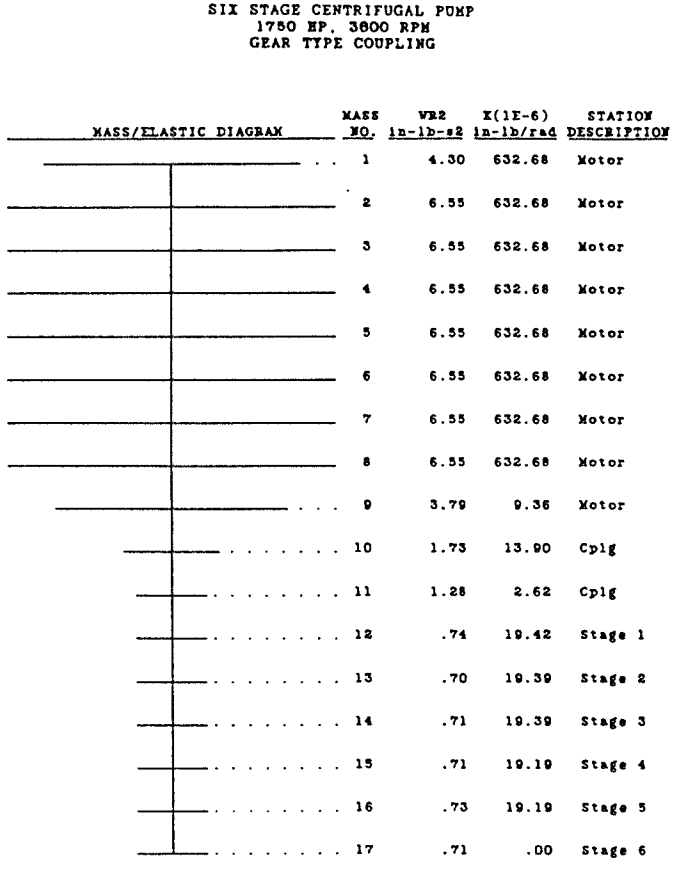

Figure 18-24. Mass-elastic diagram of six-stage pump train.

Parametric variations of the coupling stiffness should be made if changes are necessary, because most torsional problems can be solved by coupling changes.

An interference diagram for the six-stage pipeline pump is given in Figure 18-26. In this system, excitation by several orders is possible as the pump is started; however, operation at 3,600 rpm has an adequate margin from the critical speeds. Once the system has been modeled and the natural frequencies have been determined, potential forcing functions should be identified. The forcing functions represent dynamic torques applied at locations in the system that are likely to generate torque varia-

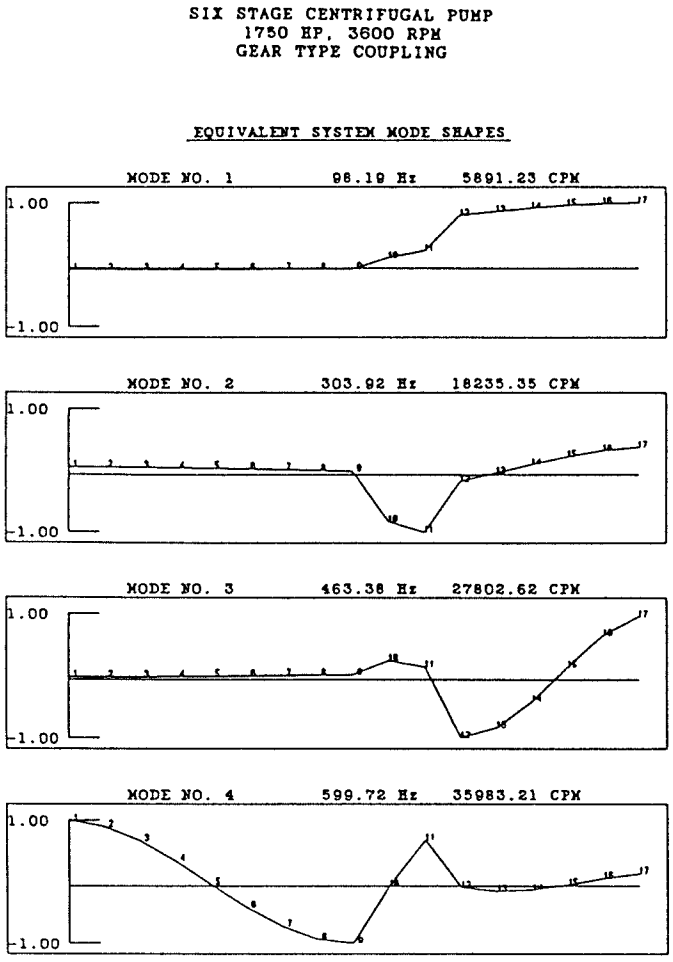

Figure 18-25. Torsional resonant mode shapes of six-stage pump train.

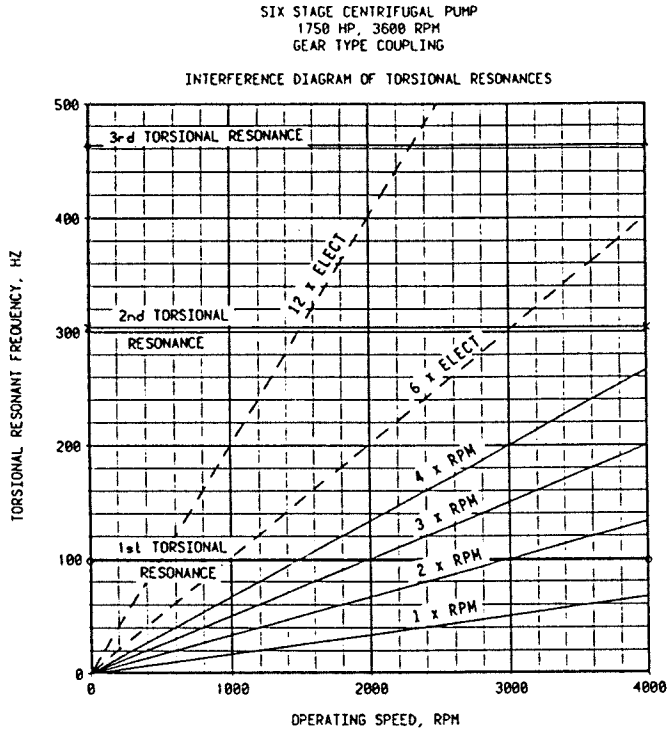

Figure 18-26. Interference diagram of torsional resonances of six-stage pump train.

tions. Identification of all possible sources of dynamic energy is an important step in diagnosing an existing vibration problem or avoiding problems at the design stage.

The most likely sources of dynamic torques include the following:

- Pumps, turbines, and compressors
- Motors (synchronous and induction)
- Couplings
- Gears
- Fluid interaction (pulsations)
- Load variations

The transient torques of a synchronous motor were measured during startup (Figure 18-27) by attaching a strain gauge to the motor shaft and obtaining the signal with an FM telemetry system. A synchronous motor produces a pulsating torque [39] that varies from twice line frequency as

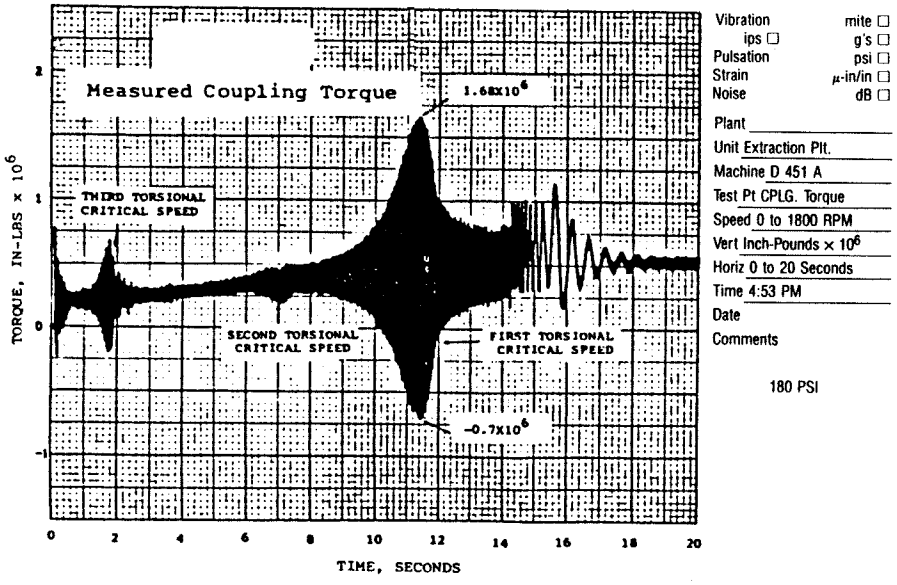

Figure 18-27. Measured coupling torque during synchronous motor startup.

it starts to zero frequency when it is synchronized with the line at operating speed.

Reliability Criteria. The overall system reliability depends upon the location of the torsional natural frequencies with regard to the potential excitation frequencies. An interference diagram generated for each system helps to identify coincidences between expected excitation frequencies and torsional natural frequencies within the operating speed range. Whenever practical, the coupling torsional stiffness and inertia properties should be selected to avoid any interferences within the desired speed range. If resonances cannot be avoided, coupling selection can be optimized based on torsional shaft stress calculations as well as location of critical speeds.

When coupling changes are implemented that have different weights than the vendor originally specified, the lateral critical speeds may be affected. Generally, heavier couplings lower the lateral critical speeds, while lighter couplings raise them. The lateral critical speeds should be reviewed to evaluate the possibility of operating near a lateral response that could result in high radial vibrations.

The acceptability of the torsional system is determined by comparison to typical engineering criteria. Common criteria used for industrial machinery (API Standards) recommend separation of the torsional critical

speed and the frequency of all driving energy by a margin of 10%. The effect of the torque modulation on coupling life should be compared to the manufacturer's vibratory torque criterion.

Allowable Torsional Stresses. For long-term reliability, torsional shaft stresses should be compared to applicable criteria. The allowable shaft stress values given by Military Standard 167 [41] are appropriate for most rotating equipment. The Military Standard 167 defines an allowable endurance limit stress of 4,000 psi zero-peak or 8,000 psi peak-peak, based on 100,000 psi ultimate tensile strength shaft material. The general equation for allowable zero-peak endurance limit is the ultimate tensile strength divided by 25.

When comparing calculated stresses to allowable stress values, the appropriate stress concentration factor and a safety factor must be used. Generally a safety factor of 2 is used for fatigue analysis. The standard keyway (USA Standard ANSI B17.1) has a stress concentration factor of 3 [42]. When these factors are used, it can be shown that fairly low levels of torsional stress can cause failures. A typical torsional stress allowable thus becomes the ultimate tensile strength divided by 150.

To evaluate the stresses at resonance, the expected torsional excitation must be applied to the system. For systems with gear boxes, a torque modulation of 1%, zero-peak is a representative torque value that has proven to be appropriate for most industrial machinery trains. As a rule of thumb, excitations at the higher orders for gears are inversely proportional to the order numbers: the second order excitation is 0.5%, the third is 0.33%, etc.

The torque excitation should be applied at the appropriate location and the torsional stresses calculated on the resonant frequencies and at the running speed. An example of the stress calculations of the first natural frequency resonance for the six-stage pump are given in Table 18-4. The maximum stresses occurred at 2,946 rpm on startup as the second order matched the first critical speed. The stresses at 3,600 rpm were low because there was a margin of approximately 17% from the nearest natural frequency. The torque excitation at the second order would cause a maximum torsional stress of 395 psi peak-peak in shaft 11, which is the pump input shaft between the coupling and the first stage impeller. The dynamic torque modulation across the couplings was calculated for the applied input modulation. For this mode, the maximum torsional vibrations occur across the coupling and the dynamic torque modulation was 48 ft-lbs.

Table 18-4
Six-Stage Centrifugal Pump
1750 HP, 3600 RPM
Gear Type Coupling

Dynamic Torques (1 Percent Zero-Peak) Applied at Motor
Maximum Resultant Torsional Stresses at 2945.62 RPM

Shaft	Stress PSI P-P	SCF	Stress PSI P-P
1	.99	2.00	1.98
2	2.47	2.00	4.93
3	3.87	2.00	7.74
4	5.21	2.00	10.41
5	6.51	2.00	13.02
6	7.82	2.00	15.65
7	9.16	2.00	18.32
8	10.52	2.00	21.03
9	130.49	3.00	391.47
10	*DYNAMIC TORQUE VARIATION*		**48.32***
11	131.77	3.00	395.30
12	72.65	2.00	145.30
13	59.57	2.00	119.13
14	45.51	2.00	91.03
15	30.84	2.00	61.68
16	15.31	2.00	30.63

* — *Values are dynamic torque variation across coupling, ft-lbs*

Variable Speed Drives

Systems that incorporate variable frequency drives [43] require additional considerations in the design stage over conventional constant speed equipment. The wide speed range increases the likelihood that at some operating speed a coincidence between a torsional natural frequency and an expected excitation frequency will exist. In addition to the fundamental mechanical frequency (motor speed), excitation frequencies include the fundamental electrical frequency (number of pole pairs times motor speed) and the sixth and twelfth orders of electrical frequency [44]. The variable frequency power supply introduces a pulsating torque with strong sixth and twelfth order harmonics.

As an example, the same six-stage pump system (described in Figure 18-24) was analyzed for a variable frequency drive motor. The dashed line in Figure 18-26 represents the sixth harmonic speed line that shows that the sixth order would excite the first torsional natural frequency at 982 rpm.

Because of the strong sixth order electrical torques produced by the variable frequency drive, the stresses (Table 18-5) are significantly greater than the stresses for the same system with a constant speed motor (compare with Table 18-4). Even though the natural frequencies of the rotor system remain constant, the exciting torques are greater and occur at a different speed.

It is dffficult to remove all coincidence of resonances with the excitation sources over a wide speed range; therefore, stress calculations must be made to evaluate the adequacy of the system response. The input shaft stresses for the six-stage pump with a variable frequency drive are shown in Figure 18-28. They are significantly different stresses than for the constant speed motor. This example demonstrates that converting a constant speed system (motor or turbine) to a variable frequency drive motor must be considered carefully. Although the variable speed provides greater efficiency; adjustments may be required (i.e., proper choice of couplings) to obtain acceptable torsional response.

Some variable speed systems use couplings with flexible elements to increase the damping as critical speeds are passed. Several couplings in common use have rubber elements to add damping that increases stiffness with higher transmitted torque. Other couplings use flexible grids or springs that again have an increased stiffness with load. These couplings are sometimes necessary when several torsional frequencies occur within the speed range. The torsional stiffness of these nonlinear couplings changes with load (transmitted torque) and speed. This nonlinearity adds complexity to the analysis. The pump load must be considered which also varies as a function of speed squared.

Diagnosis of Pump Vibration Problems

Large plants that handle liquids (i.e., chemical plants) may have hundreds or more small pumps, making it almost impossible to measure each pump in detail on a regular basis. The cost of a detailed analysis with several transducers, spectrum analyses, and the necessary study of the data can quickly exceed the cost of repair or even replacement of some of the small pumps. Only the pumps in a critical system, which could affect production if a failure occurred, can afford the expense of a detailed analysis or a permanent monitoring system. However, the hundreds of small pumps need regular attention to keep plant efficiency (and flow rates) from dropping.

An effective preventative maintenance program should periodically measure and record the vibrations on each bearing of the pump and its driver. Measurements with a hand-held velocity transducer or data collector system are usually adequate to obtain periodic data to evaluate the

Table 18-5
Six-Stage Centrifugal Pump
1750 HP, 3600 RPM Variable Frequency Drive Motor
Gear Type Coupling

Shaft	Stress PSI P-P	SCF	Stress PSI P-P
	Dynamic Torques (1 Percent Zero-Peak) Applied at Motor Maximum Resultant Torsional Stresses at 981.87 RPM		
1	48.12	2.00	96.25
2	121.31	2.00	242.62
3	193.97	2.00	387.93
4	265.92	2.00	531.84
5	336.94	2.00	673.89
6	406.63	2.00	813.26
7	474.66	2.00	949.32
8	540.76	2.00	1081.52
9	6676.68	3.00	20030.04
10	*DYNAMIC TORQUE VARIATION*		**2489.59***
11	6822.28	3.00	20466.84
12	3763.91	2.00	7527.81
13	3087.43	2.00	6174.85
14	2359.91	2.00	4719.81
15	1599.41	2.00	3198.81
16	794.30	2.00	1588.60

* —*Values are dynamic torque variation across coupling, ft-lbs*

vibrational trend. If the vibrations show an increasing trend, the unit should be monitored more frequently. Vibrational guidelines in common usage can aid in determining the severity or extent of damage so that maintenance can be scheduled. A vibrational velocity of less than 0.3 ips (inches per second) is generally accepted as satisfactory operation for pumps [7] and motors. Velocity levels above 0.3 ips are warnings of potential problems. Velocity levels of 0.5 ips and above may be indicative of significant damage to the bearings, seals, or rotor.

The basis of troubleshooting is obtaining test data on troublesome pumps during normal operation and comparing the data to the purchase specifications, vendor guarantees, or applicable vibration criteria. It is crucial to the success of the troubleshooting effort to have adequate instrumentation on the pump system. In many cases, the instrumentation can be temporarily added to obtain the required measurements.

Measurement Techniques

Typically pumps are installed with a minimum of vibration monitoring equipment. Some pumps may have a velocity pickup on each bearing

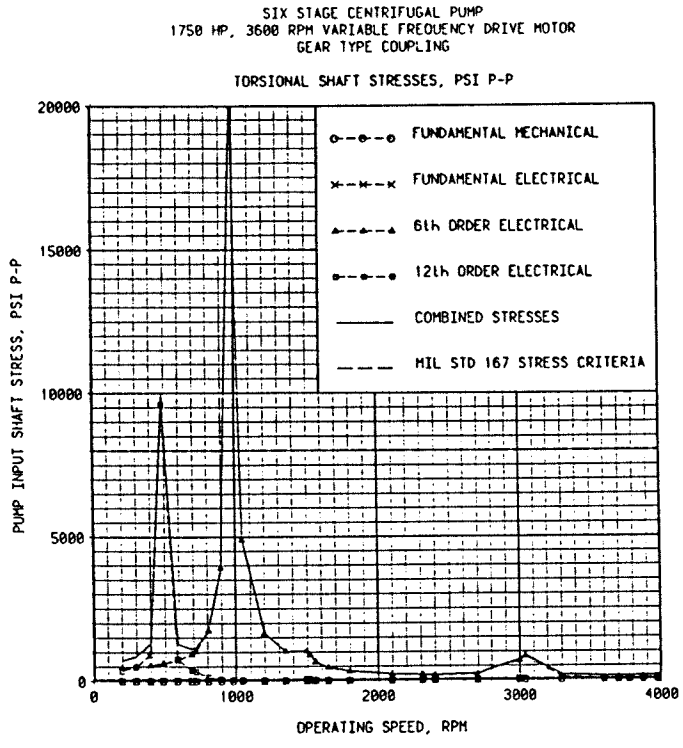

Figure 18-28. Pump shaft stress with variable frequency drive motor.

housing. These systems are satisfactory for pumps with rolling element bearings, because the bearings transmit the rotor forces directly to the case. However, additional instrumentation is often required to define difficult problems. For pumps with oil film bearings, it is desirable to have two proximity probes 90° apart near each bearing and an axial probe. Accelerometers and velocity probes attached to the bearing housings or case are often used to measure pump vibration; however, if the proximity probes are not installed, the data will be limited and may be a detriment to the diagnosis of some types of problems. A pressure transducer is vital to diagnostic work for measuring dynamic pulsations in the piping, impeller eye, diffuser, and across flow meters. Accurate flow measurements are necessary to define the pump vibration characteristics as a function of its location on the head-flow performance map.

Accelerometers or velocity transducers can be used to determine frequencies and amplitudes of the pump case or support structure during normal operation [45]. Two accelerometers and a dual channel oscilloscope displaying their complex vibration waveforms can be used to de-

fine the phase relationship between the signals. By keeping one accelerometer stationary as a reference, subsequent moves of the other accelerometer to measure amplitudes at various points on the structure can define the mode shape. This method requires that the speed remain constant while the measurements are being made. The speed should be set at the resonant mode to be identified.

As a general technique, this type of measurement should be taken at the resonant frequencies near the operating speed to define the components that control the resonance. Measurements can also be made by using a reference accelerometer on the structure to trigger the data loading sequence of a real time analyzer to enable more accurate amplitude/phase data to be taken. The reference signal may be from a key phase signal that relates the vibrational maximum to the actual shaft position.

Amplitude/phase data for a feedwater pump (Figure 18-29) is tabulated directly on the figure to aid in interpreting the mode shape. The vertical vibrations at the pump centerline are plotted in Figure 18-29a. Although the phase difference from the outboard and inboard ends was 165° (not 180°), the mode was characterized by a rocking motion about the pivotal axis. The vertical vibrations on the pump inboard (Figure 18-29b) indicate that the horizontal support beam was one of the main flexible elements.

Impact Tests

An impact test is a simple technique that can be used to excite resonances of flexible substructures. A significant advantage of the method is that mechanical natural frequencies can be measured while units are down. Typical instrumentation includes an accelerometer attached to the head of a rubber-tipped hammer to measure the impact force and a second accelerometer used to measure the response of the test structure. In modal analysis testing, the accelerometer remains at one location and an impact hammer is used to excite the structure at selected locations. The response signal can be automatically divided by the impact signal using a fast fourier transform (FFT) spectrum analyzer with transfer function (XFR) capabilities.

For best results, the impact velocity should not be greatly different from the vibrational velocity of the vibrating member. For example, the lowest beam mode of a piping span can be excited with a rubber mallet by applying the impact with a forceful, medium-speed swing. However, a sharp rap with a steel-faced hammer could produce higher modes of beam vibration or possibly a pipe shell wall resonance. These higher energy modes will be quickly damped and difficult to identify. Using modal

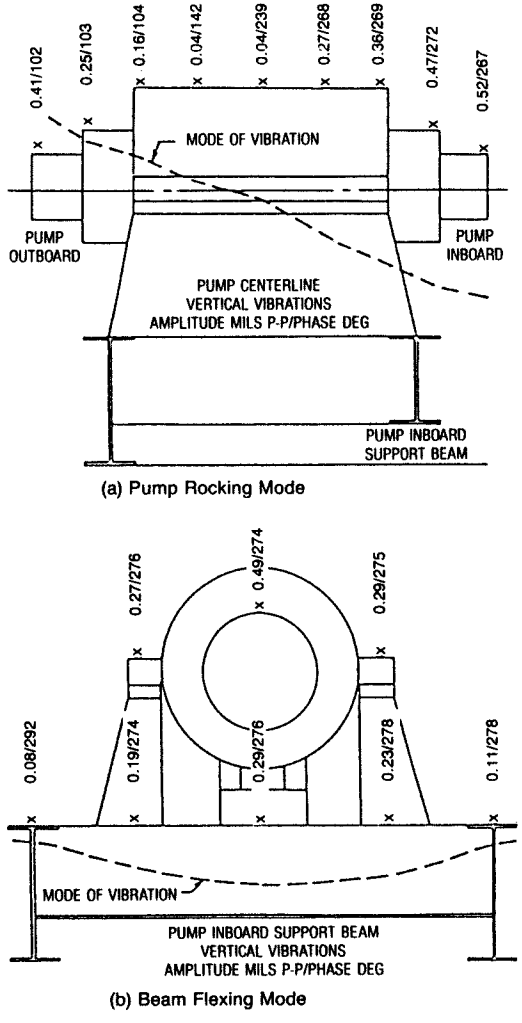

Figure 18-29. Pump vibrational mode shapes during operation.

analysis techniques, the input spectrum can be evaluated and the impact can be adjusted to obtain the best results for the structure being tested.

In nonsymmetrical members or structures, a resonant mode has a preferred direction of motion. Impact testing should be approached on an experimental basis by trying variations of impact velocity, direction, etc. Numerous frequencies may occur that make the mode shapes difficult to identify. Generally, the lower modes of vibration will be predominate. The mode of vibration is strongly influenced by the following:

- Direction of impact
- Interface material
- Impact velocity
- Contact time
- Impact location

The objective of the testing should be to identify structural resonant frequencies that occur within the machinery operating frequency range. In a complex system, there are many natural frequencies. Consequently, it may be difficult to identify the individual natural frequencies because the vibrations can be transmitted between the different elements (pump rotor, case, and support structure). The impact technique is useful for separating the structural natural frequencies because each element can be impacted individually. Individual resonances can generally be identified by analyzing the vibrational mode shapes and comparing the transfer function amplitudes.

The transfer function amplitude is an indication of the relative stiffness of a structure. For example, a rigid structure that is difficult to excite or resonate would have a low amplitude transfer function (response/force). A highly responsive structure would have a higher amplitude transfer function because less force is required to obtain the response. This technique was used to determine the bearing housing resonance of a pump that is described in the case histories that follow.

Various types of data presentation formats are in common use and are described in the case histories. The data format is dependent upon the type of instrumentation available; however, for convenience of comparison to criteria or specifications, some formats may be more convenient than others.

Troubleshooting

As examples of the types of diagnostic procedures that are used to identify the causes of some typical pump problems, several field case histories will be presented.

Bearing Housing Resonance of Feed Charge Pumps. High vibration amplitudes and seal failures occurred on one of a pair of centrifugal pumps that are the feed charge pumps for a cat feed hydro-treater plant. The pumps were driven by electric motors at a speed of approximately 3,587 rpm (59.8 Hz). The pumps have five impellers; the first two impellers have six vanes and the last three impellers have seven vanes.

Vibration data recorded on both pumps indicated that the vibration levels were significantly higher on the inboard bearing of Pump A. The maximum vibration occurred at seven times running speed (418 Hz) which is the vane passing frequency of the last three impellers.

The high vibration levels and seal failures on the inboard bearing of the pump could be caused by several problems, including:

- Pulsation at the vane passing frequency that can increase the forces on the impeller and shaft.
- Mechanical or structural natural frequencies that amplify the vibration levels.
- Misalignment between the motor and the pump or internal misalignment between the pump bearings.

A field test was performed to measure the vibrations and pulsations in the system. The vibration amplitudes were considerably higher on the inboard bearing of Pump A which experienced the seal failures. The vibration amplitude increased significantly between the case and the bearing housing. This differential vibration could be the cause of the seal failures. The bearing housing vibrations of Pump A were primarily at seven times running speed (418 Hz).

Vibration measurements were taken at four locations between the end of the case and the end of the bearing to illustrate the vibration mode shapes. The vibration amplitudes on the inboard bearing were considerably higher near the end of the bearing housing compared to near the case. The horizontal vibrational mode can be defined from the vibration spectra at the four points shown in Figure 18-30. As shown, there was significant differential motion between the case and the end of the flange and across the bolted flange. The vibration amplitude on the bearing housing was approximately 6 g peak-peak at 418 Hz (0.44 in./sec peak). Most allowable vibration criteria would consider these amplitudes to be excessive. However, the actual differential displacement was only 0.13 mils peak-peak. The amplitudes at the outboard bearing were lower compared to the amplitudes on the inboard bearing.

The discharge pulsation amplitudes were 12 psi at seven times running speed and 3 psi at fourteen times running speed. The discharge pulsations were higher on Pump B (without any seal failures), which indicated that the pulsations were not the cause of the increased vibrations.

Impact Tests

Impact tests on the bearing housings indicated that the inboard bearing housings were very responsive compared to the outboard bearing hous-

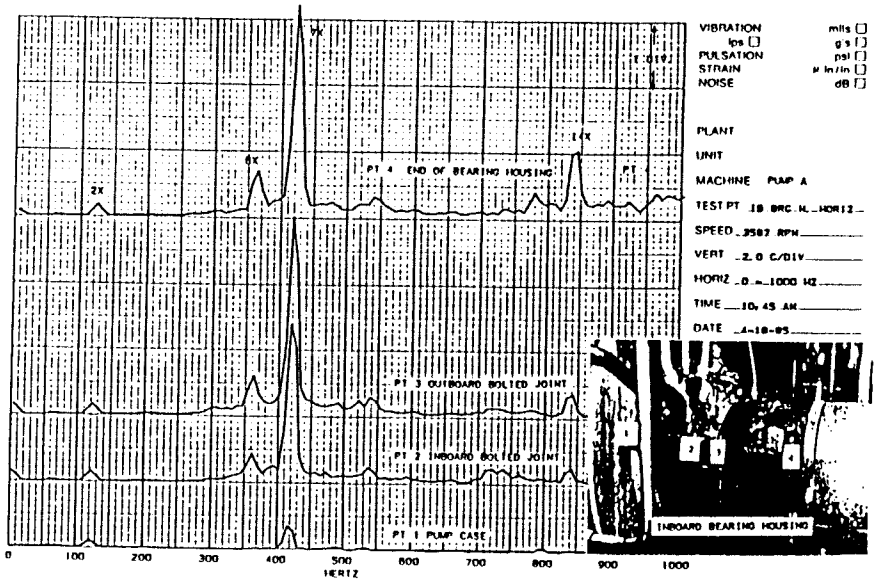

Figure 18-30. Vibrational response of inboard bearing housing.

ings. The transfer function (Figure 18-31) was plotted with a full scale amplitude equal to 0.4 (0.05 per major division on the graph paper).

The inboard bearing of Pump A had a major response at 420 Hz with a transfer function amplitude of 0.24. This frequency was almost coincident with seven times running speed (418 Hz) which would amplify the vibration levels at seven times running speed and appeared to be the primary cause of the high vibration at seven times running speed. The flange bolts were tightened and the frequency increased to 430 Hz which indicated that the response near 420 Hz was primarily associated with the bearing housing and its attachment stiffness to the case.

A similar major response near 432 Hz occurred in the vertical direction. The transfer function amplitude was lower and the frequency was higher than measured in the horizontal direction because the bearing was slightly stiffer in the vertical direction compared to the horizontal direction. When the flange bolts were tightened, the response near 432 Hz was increased to 440 Hz.

The outboard bearing was more massive and stiffer and not as responsive as the inboard bearing. There were no major responses in the horizontal direction near the excitation frequencies of interest. A vertical response was measured near 580 Hz; however, because it was above the frequencies of interest, it should not cause an increase in vibration on the bearing housings.

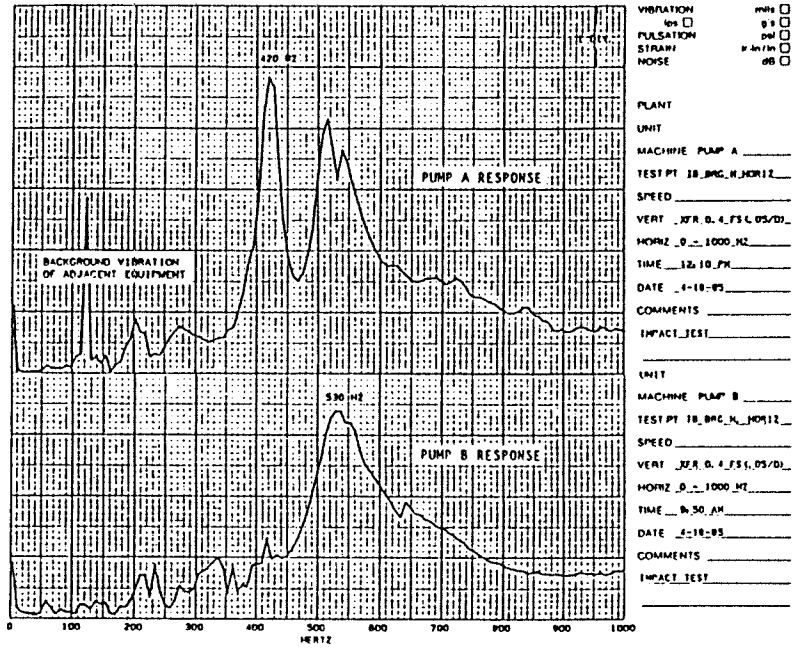

Figure 18-31. Structural natural frequency of inboard bearing housing.

Impact tests were performed on Pump B (no seal failures). The responses on the inboard bearing were 530 Hz in the horizontal direction (Figure 18-31) and 600 Hz in the vertical direction. Although visually the two pumps appeared to be identical, detailed measurements revealed slight differences in the cross-sectional thickness and lengths of the inboard support between the flange and the end of the cases. Apparently these slight dimensional differences caused the mechanical natural frequencies to vary considerably between the two pumps.

The obvious solution to the problem would be to replace the bearing housing casting or modify the inboard bearing housing support of Pump A. The mechanical natural frequency could be increased by stiffening the support with gussets. For improved reliability, the mechanical natural frequency should be increased approximately 10% above the primary excitation frequency at seven times running speed.

Pump Critical Speed Problem [46]. A critical speed analysis was performed on a centrifugal pump used as a jetting pump on a pipe laying barge. The predicted unbalanced vibration response of the centrifugal pump showing the effects of the seals is shown in Figure 18-32. Note that

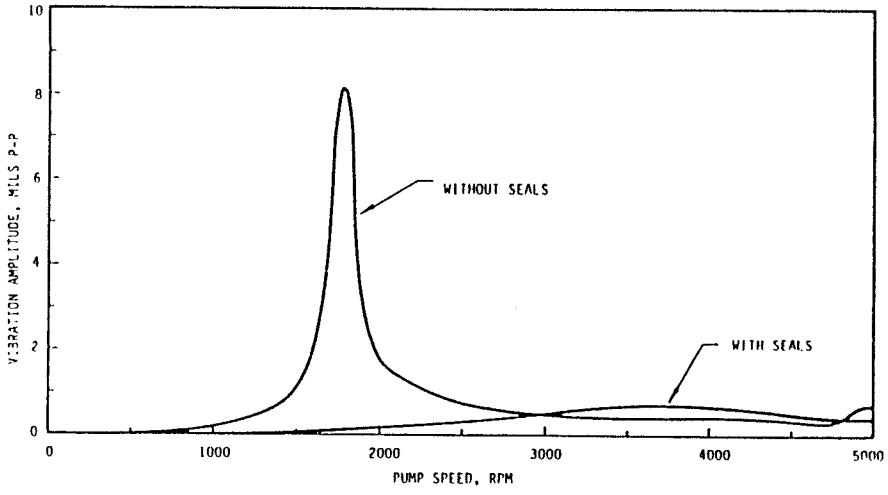

Figure 18-32. Predicted vibration of three-stage centrifugal pump showing effect of seals.

the seal effects shifted the critical speed from 1,800 to 3,700 rpm and significantly increased the damping, which illustrates that the pump critical speed should be sensitive to seal stiffness effects. When the seals were considered, the predicted amplitudes were reduced by a factor of more than 10 to 1.

The vibrations on the pump were measured (Figure 18-33) using the peak-store capabilities of a real-time analyzer. The vibrations were low until the pump reached 3,300 rpm and then sharply increased to 6 mils peak-peak at 3,600 rpm. The design speed was 3,600 rpm; however, the pump could not run continuously at that speed. The pump speed was kept below 3,400 rpm so that the vibrations were less than 2 mils peak-peak. Even with the reduced pump speed, the pipe-laying barge was able to set pipe-laying records.

After a year of operation, the pump vibrations began to increase until the vibrations at 3,400 rpm were unacceptable. The pressure breakdown bushing had worn which reduced its effective stiffness and the critical speed had dropped to 3,400 rpm. It was recommended that the pump be operated at a speed above the critical speed. This was tried and the pump operated at 3,600 rpm with vibration levels less than 2 mils peak-peak. The barge remained in service and reset the pipe-laying records during the next season.

The data analysis technique used to determine this critical speed was to use the peak-store capabilities of the real-time analyzer. An alternate method would be to use a tracking filter to determine the critical speed

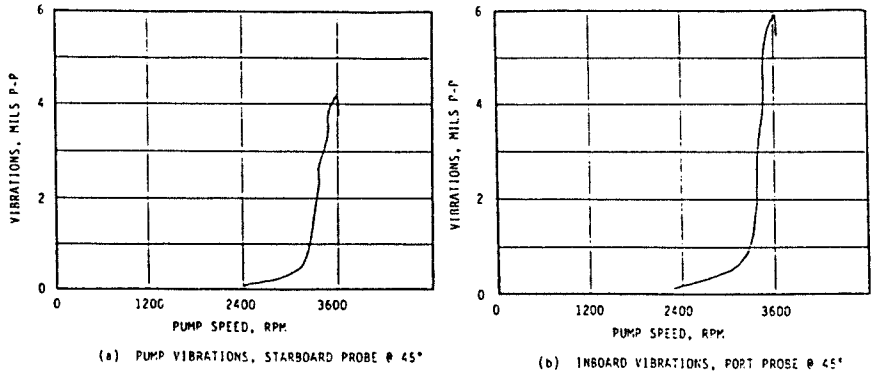

Figure 18-33. Jetting pump measured vibrations.

response because both the amplitude and phase data could be made available. Although it is generally better to have both the Bode and Nyquist plots, for this case they were not required to define the cause of the vibration plot.

High Vibrations of a Centrifugal Pump. Critical speed calculations were performed on a three-stage centrifugal pump to determine if a critical speed existed near running speed. The mode shape calculations for the first and second critical speeds are summarized in Figures 18-34 and 18-35. As discussed, the liquid seals can significantly affect the critical speeds of a pump; however, for this rotor, the seals only increased the critical speed by about 15%. This critical speed analysis considered a shaft with two bearings and the eight seals, or ten sets of stiffness and damping coefficients. Each of these coefficients varied as a function of speed and was included in the unbalanced response analysis (Figure 18-36). A comparison of predicted responses to measured test stand data is given in Figure 18-37. The agreement with the measured data was considered good, indicating that the rotordynamic model of the rotor and the bearing and seal clearances was acceptable.

A data acquisition system with a tracking filter was used to plot the amplitude and phase angle versus speed (Bode Plot). The lack of a significant phase shift through the critical speed could not be explained without a more detailed analysis. As in many field studies, other priorities prevailed, and additional tests were not possible. Although the critical speed was in the running speed range, the vibration amplitudes were low and any wear of the seals should move it further away from the rated speed of 3,600 rpm.

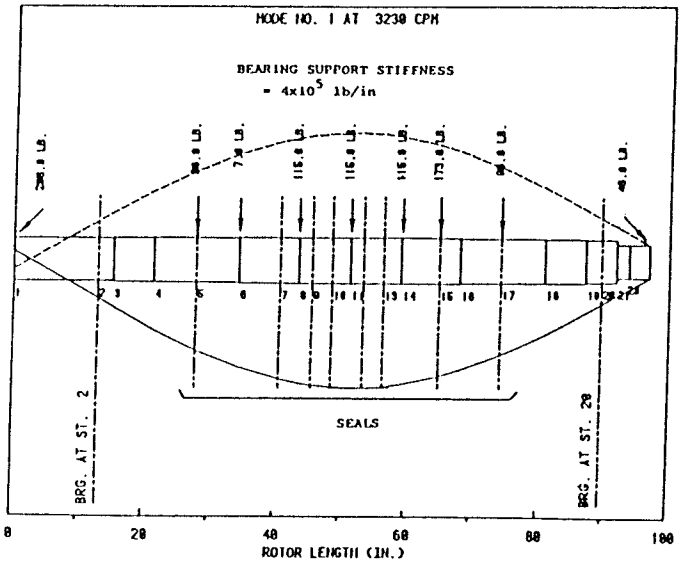

Figure 18-34. Three-stage pump—first mode response—with seals.

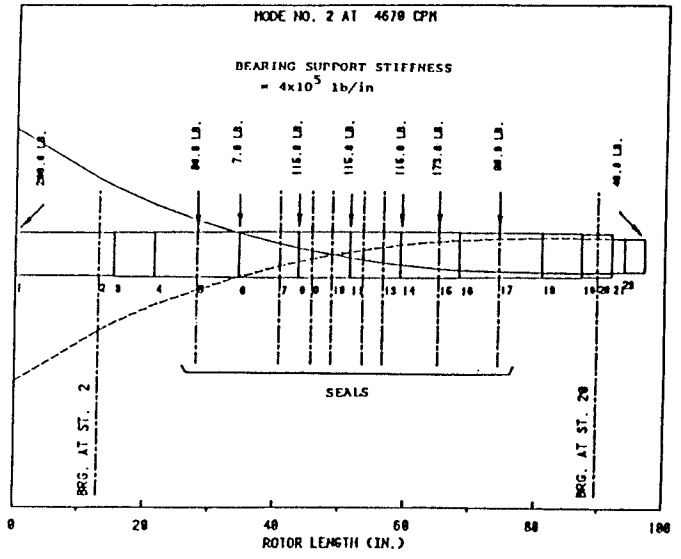

Figure 18-35. Three-stage pump—second mode response—with seals.

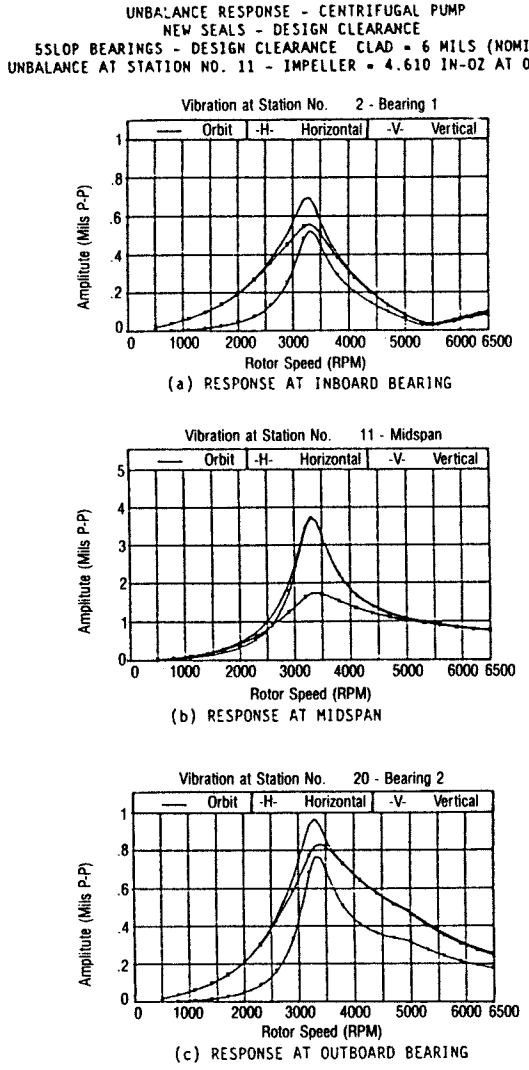

Figure 18-36. Three-stage pump—unbalanced response—with seals.

Pulsation Induced Vibrations [14]. A four-stage centrifugal pump suffered repeated failures of the splitter between pump stages. A detailed field study revealed the cause of the problems to be an acoustic resonance of the long cross-over that connected the second-stage discharge with the third-stage suction (Figure 18-38). The resonant frequency was a half-wave acoustic resonance.

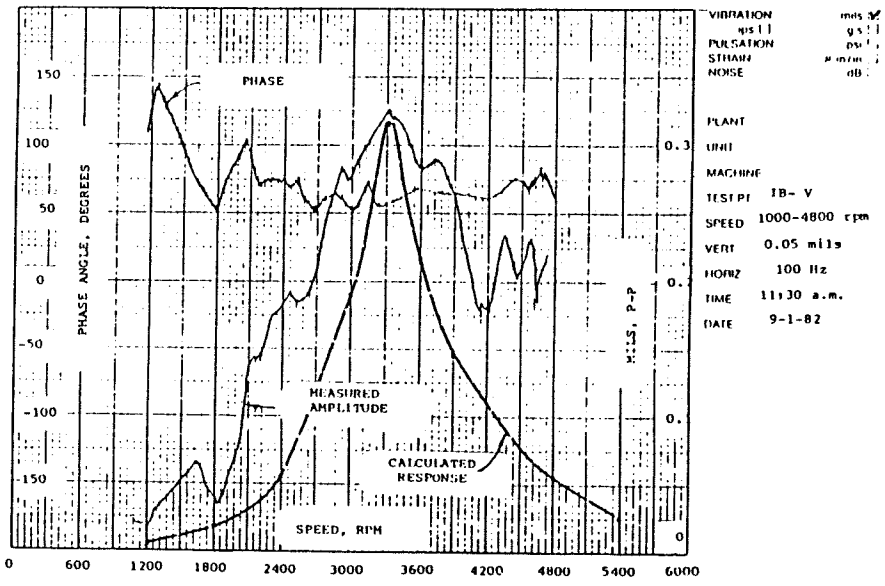

Figure 18-37. Three-stage pump—comparison of measured and calculated response.

$$f = \frac{c}{2 \times L}$$

where: c = acoustic velocity, ft/sec
L = length, ft

The speed of sound in water is a function of the temperature, and at 310°F was calculated to be 4,770 ft/sec. The length of the cross-over was 5.75 ft. The acoustic natural frequency was

$$f = \frac{4770}{2 \times 5.75} = 415\text{Hz}$$

The acoustic resonant frequency was excited by the vane passing frequency (seven times running speed). Coincidence occurred at (415) (60)/ 7 = 3,560 rpm.

Dynamic pressure measurements in the center of the cross-over showed pulsation amplitudes of 100 psi peak-to-peak. The pulsations at the suction and discharge flanges were less than 10 psi peak-to-peak, which agreed with the mode shape of the half-wave acoustic resonance.

There were two possible changes that could eliminate the coincidence of vane passing frequency with the resonant frequency and reduce the

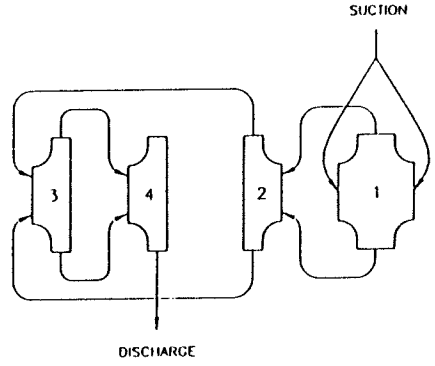

Figure 18-38. Flow schematic of a four-stage pump.

vibration levels that occurred at a speed of 3,560 rpm. One possible change was to increase the vane tip clearance to minimize the turbulence that produces the pulsations. This modification would require trimming the diameter of the impellers and operating the pump at a higher speed to attain the capacity. Another possibility was to change to a six- or eight-vane impeller to alter the vane passing frequency. The impeller diameter modification was the quickest and most economical and was carried out in the field, and the splitter failures were eliminated.

This example also illustrates the importance of selecting proper test points when measuring pulsations. For example, if an acoustical resonance is expected in the cross-over, then the pressure transducer should be installed near the center of the cross-over length rather than at the ends.

Sometimes the cross-over or cross-under passage can have an acoustical resonance that can be so severe that it can excite the shaft and result in high shaft vibrations [46]. This is illustrated for a different pump problem (Figure 18-39) which had shaft vibrations at operating speed (3,400 rpm) of 1 mil peak-peak and vibrations at five times speed of 0.5 mils peak-peak. Pulsation levels in the cross-under were over 250 psi and caused approximately 0.5 mils peak-peak of shaft vibration at the acoustic natural frequency.

Shaft Failures Caused by Hydraulic Forces. Repeated shaft bending fatigue failures were experienced in a single stage overhung high-pressure water pump. The failures exhibited the classical fatigue beach marks with the failures occurring straight across the shaft at the sharp corner at the change in diameter. The pump was instrumented with proximity probes, pressure transducers, and accelerometers. Measurements were made

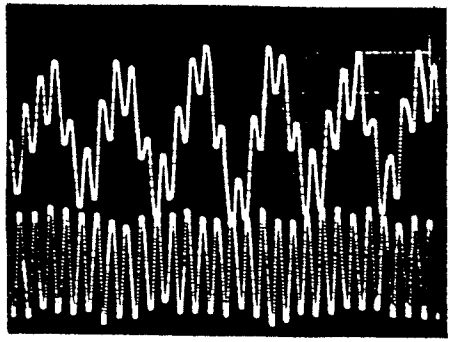

Figure 18-39. Shaft vibrations caused by acoustic resonance.

over a wide range of startup and flow conditions. The pumps had a double-volute casing that was supposed to balance the radial forces on the impeller; however, measurements made of the shaft centerline by measuring the DC voltage on the proximity probes showed that the impeller was being forced upward against the casing. This caused a large bending moment on the shaft as it rotated. The pump shaft center location near the bearings was displayed on an oscilloscope (Figure 18-40) during startup and during recycle. A differential movement of 6 mils occurred across a short distance along the shaft. The wear patterns on the impellers were consistent with the major axis of the orbit and the direction that the shaft moved. The large movement in the bearing journals only occurred under certain start-up conditions; therefore, it was possible to modify the start-up procedures to ensure that the large hydraulic forces would not cause shaft failures.

Hydraulic forces can cause shaft failures as illustrated by this example; therefore, it is good practice to determine if the shaft is properly aligned in its journals under all operating conditions.

Pump Instability Problem. A high speed pump experienced high vibrations in the process of startup at the plant site. Originally, the problem was thought to be due to a lateral critical speed causing increased synchronous vibration levels when full speed was reached.

Analysis of this problem was particularly difficult due to the extremely short startup time of the motor-driven pump and the even more rapid rate at which the vibration levels increased as the pump approached rated speed. To analyze the problem, an FM recording of a startup was analyzed while running the recorder playback at 1/8 of recorded speed, which in effect, caused the startup period during playback to be eight

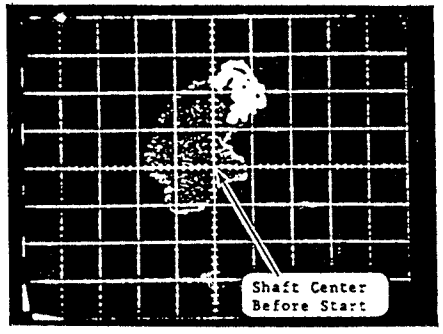

(a) PUMP SHAFT MIDSPAN SPATIAL POSITION

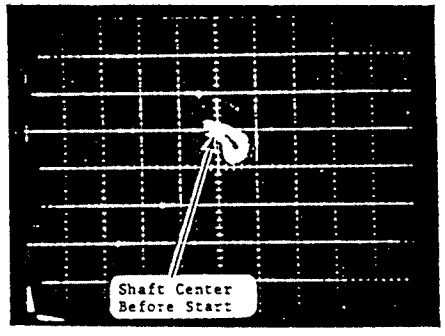

(b) PUMP SHAFT INBOARD SPATIAL POSITION

Figure 18-40. Pump shaft vibration orbits.

times as long. A cascade plot of the vibration data (Figure 18-41) showed that just before trip of the unit at 21,960 rpm, an instability vibration component occurred near 15,000 cpm. From this and other data, it was determined that the high vibrations were caused by:

- A sudden increase in nonsynchronous vibration as the unit approached full speed resulting in shaft bow.
- A sudden increase in unbalance due to the shaft bow and as a result, a rapid increase in synchronous vibration levels as the nonsynchronous components disappeared.

After the problem source was identified using the above data analysis technique, computer simulation of the rotor led to a solution consisting of bearing modifications. The stability analysis of the pump rotor predicted that the pump had an unstable mode at 15,000 cpm with a negative loga-

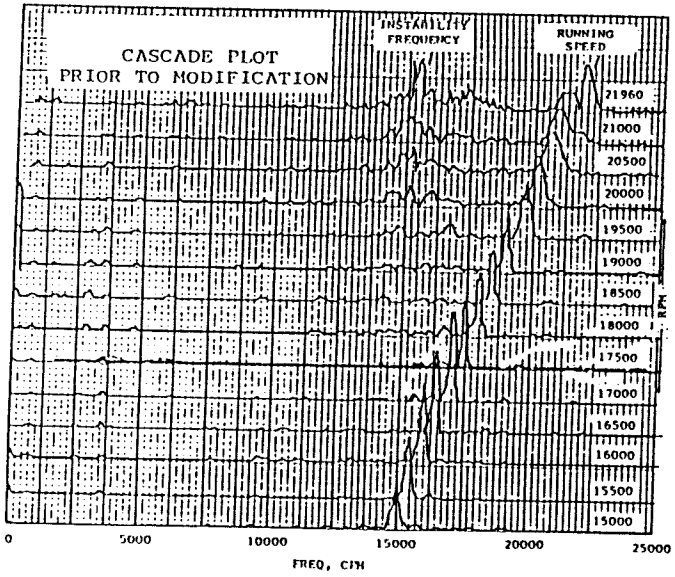

Figure 18-41. Nonsynchronous instability vibration of high speed pump.

rithmic decrement of 0.01 for a simulated fluid aerodynamic loading of 1,000 lb/in. at the impellers [36, 47]. The pump rotor with the modified bearings was predicted to have a positive logarithmic decrement of 0.10. The rotor vibrations after the bearing modifications were made are shown in Figure 18-42. The nonsynchronous vibration component was no longer present and the unit has since operated successfully.

Appendix
Acoustic Velocity of Liquids

The acoustic velocity of liquids can be written as a function of the isentropic bulk modulus, K_s and the specific gravity:

$$c = 8.615 \sqrt{\frac{K_s}{\text{sp gr}}} \qquad (1)$$

where c = acoustic velocity, ft/sec
sp gr = specific gravity
K_s = isentropic (tangent) bulk modulus, psi

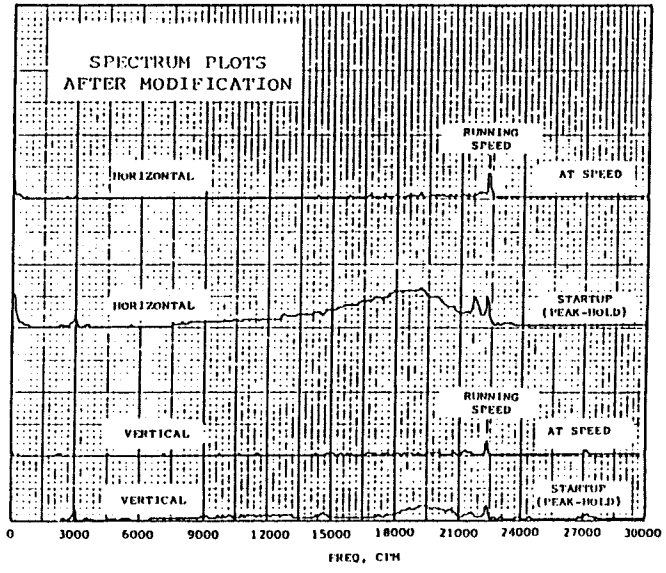

Figure 18-42. High speed pump vibrations after bearing modification.

At low pressure, water can be considered to be incompressible and the acoustic velocity is primarily dependent upon the change of density with respect to temperature. The acoustic velocity of water at low pressures [48] is given for various temperatures from 32° to 212°F in Figure 18-43. For elevated pressures, the acoustic velocity must be adjusted for pressure effects and the function using the bulk modulus is convenient.

The bulk modulus of water [49] can be calculated with the following equation for pressures up to 45,000 psig and various temperatures.

$$K_s = 1000\ K_o + 3.4P \qquad (2)$$

where K_o = constant from Table 18-6
K_s = isentropic tangent bulk modulus, psi
P = pressure psia

The calculation accuracy is ±0.5% for the isentropic bulk modulus of water at 68°F and lower pressures. The error should not exceed ±3% at elevated pressures (greater than 44,000 psi) and temperatures (greater than 212°F).

The bulk modulus for petroleum oils [50] (hydraulic fluids) can be determined for various temperatures and pressures by using Figures 18-44 and 18-45 which were developed by the API. The isothermal secant bulk modulus for petroleum oils at 20,000 psig is related to density and tem-

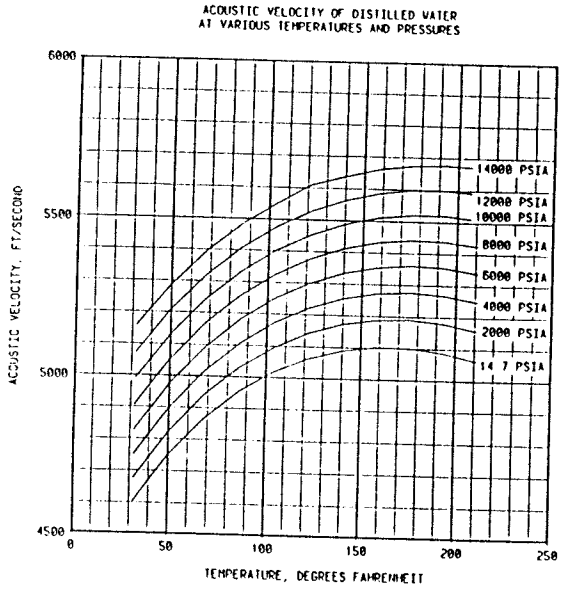

Figure 18-43. Acoustic velocity of distilled water at various temperatures and pressures.

Table 18-6 [49]
Constant K_o for Pressure Correction for Bulk Modulus of Water

$K_s = 1000\ K_o + 3.4P$
P = pressure, psia
(valid up to 45000 psia)

Temperature (°F)	Constant K_o
32	289
50	308
68	323
86	333
104	340
122	345
140	348
158	348
176	341
194	342
212	336

perature in Figure 18-44. The isothermal tangent bulk modulus has been shown to be approximately equal to the secant bulk modulus at twice the pressure within ±1%. Pressure compensation for the isothermal secant bulk modulus can be made by using Figure 18-45.

The isothermal bulk modulus, K_T, and isentropic bulk modulus, K_s, are related by the following equation:

$$K_s = K_T \frac{c_P}{c_V} \tag{3}$$

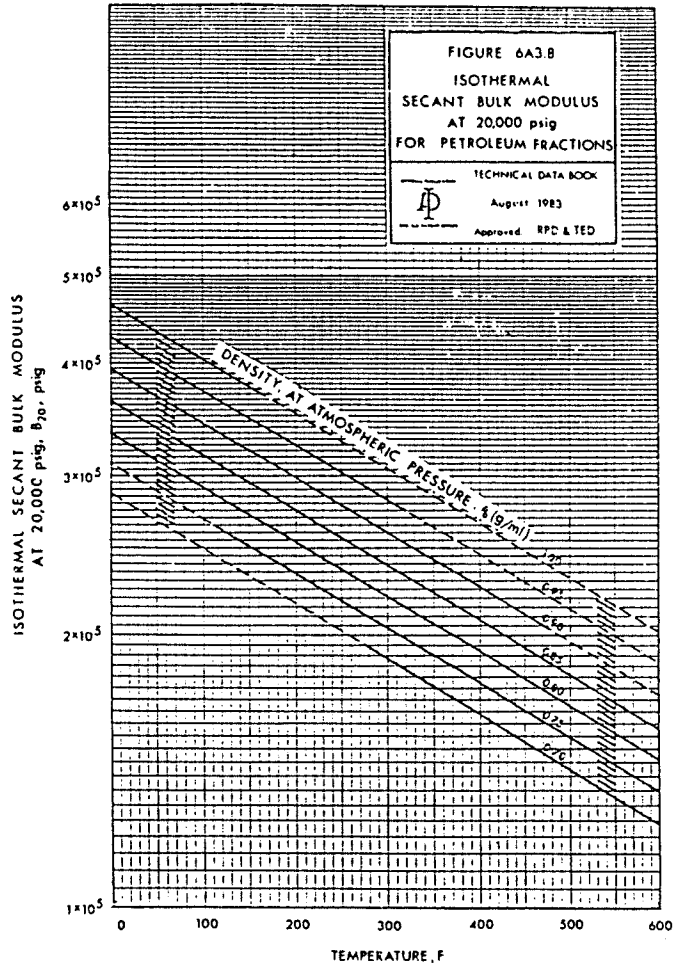

Figure 18-44. Isothermal secant bulk modulus at 20,000 psig for petroleum fractions [50].

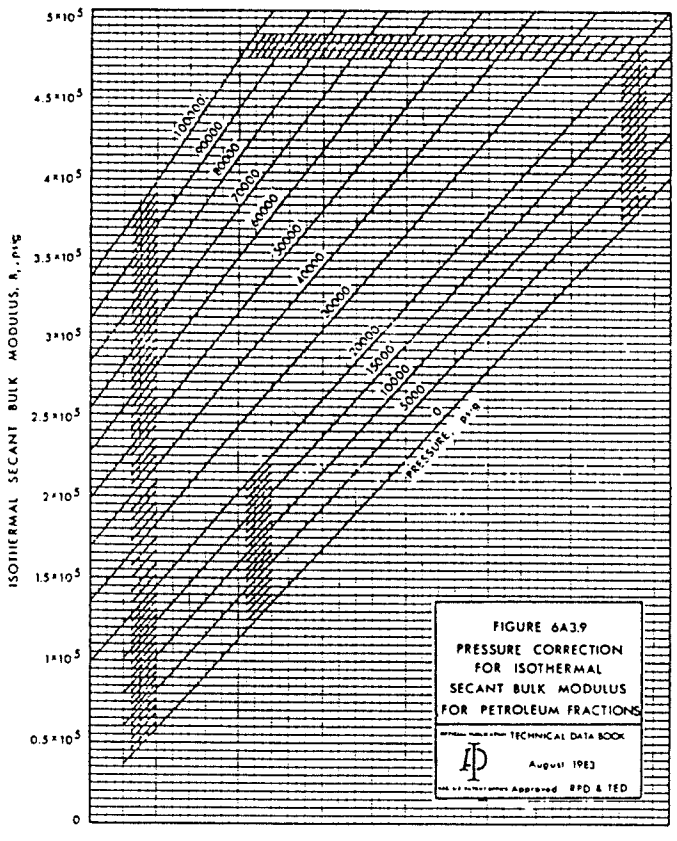

Figure 18-45. Pressure correction for isothermal secant bulk modulus for petroleum fractions [50].

The value of c_P/c_V for most hydraulic fluids is approximately 1.15.

The isentropic tangent bulk modulus for common petroleum oils can be determined from the Figures 18-44 and 18-45 as follows:

1. On Figure 18-44, enter the desired temperature on the horizontal scale and go to the proper specific gravity line to read the isothermal secant bulk modulus at the reference pressure of 20,000 psig.
2. Enter the isothermal secant bulk modulus (value from Step 1) on Figure 18-45 on the vertical scale; proceed horizontally to intersect the 20,000 psi reference pressure line; move vertically to the line corresponding to twice the desired pressure. Move horizontally to the left and read the equivalent isothermal tangent bulk modulus on the scale.
3. Multiply the isothermal tangent bulk modulus by 1.15 (to compensate for ratio of specific heats) to determine the value of the isentropic tangent bulk modulus.

The value of the isentropic tangent bulk modulus obtained in Step 3 can be used in Equation 1 to calculate the acoustic velocity.

Piping systems with incompressible fluids (liquids) have an apparent effect on the acoustic velocity because of the pipe wall flexibility. The classical Korteweg correction can be used for thin wall pipe (wall thickness $<$ 10% diameter) to adjust the acoustic velocity.

$$c_{adjusted} = c\sqrt{\frac{1}{1+\frac{DK_s}{tE}}} \tag{4}$$

where D = pipe diameter, in.
t = pipe wall thickness, in.
E = elastic modulus of pipe material, psi

References

1. Florjancic, D., Schoffler, W. and Zogg, H., "Primary Noise Abatement on Centrifugal Pumps," Sulzer Tech., Rev. 1:24, 1980.
2. Szenasi, F. R. and Wachel, J. C., Section 8.4, "Pump Noise," *Pump Handbook,* 2nd ed., McGraw-Hill, 1986, pp. 8.101–8.118.
3. Jones, A. B., "The Mathematical Theory of Rolling-Element Bearings," *Mechanical Design and Systems Handbook,* McGraw-Hill, 1964, pp. 13-1 to 13-76.
4. *Centrifugal Pump Hydraulic Instability,* CS-1445 Research Project 1266-18, Electric Power Research Institute, 3412 Hillview Ave., Palo Alto, California, 1980.
5. Wachel, J. C. and Tison, J. D., *Field Instrumentation and Diagnostics of Pump Vibration Problems,* Presented at Rotating Machinery and Controls Short Course, University of Virginia, June 6–7, 1983.
6. Mancuso, J. R., *Couplings and Joints,* Marcel Dekker, Inc., New York, 1986, pp. 340–350.
7. API Standard 610 "Centrifugal Pumps for General Refinery Services," Section 2.8, 7th ed., American Petroleum Institute, Washington, D.C., 1989.

8. Bloch, H. P., "Improving Machinery Reliability," *Practical Machinery Management for Process Plants,* Vol. I, Gulf Publishing Company, Houston, Texas, 1982, pp. 72–162.
9. Atkins, K. E., Tison, J. D. and Wachel, J. C., "Critical Speed Analysis of an Eight Stage Centrifugal Pump," *Proceedings of the Second International Pump Symposium,* April 1985, pp. 59–65.
10. Wood, D. J. and Chao, S. P. "Effect of Pipeline Junctions on Waterhammer Surges," *Proceedings of the ASCE, Transportation Engineering Journal,* August 1978, pp. 441–457.
11. Fraser, W. H., "Flow Recirculation in Centrifugal Pumps," in *Proceedings of the Tenth Turbomachinery Symposium,* 1981.
12. Fraser, W. H., "Recirculation in Centrifugal Pumps: Materials of Construction of Fluid Machinery and Their Relationship to Design and Performance," paper presented at winter annual meeting of ASME, Washington, D.C., November 16, 1982.
13. Wachel, J. C. and Szenasi, F.R., et al., "Vibrations in Reciprocating Machinery and Piping," *EDI Report 85-305,* Chapter 2, October, 1985.
14. Sparks, C. R. and Wachel, J. C., "Pulsations in Liquid Pump and Piping Systems," *Proceedings of the Fifth Turbomachinery Symposium,* October 1976, pp. 55–61.
15. Wylie, E. B. and Streeter, V. L., *Fluid Transients,* FEB Press, Ann Arbor, Michigan, 2nd Ed., pp. 213–224, 1983.
16. *Technical Data Handbook-Petroleum Refining,* Vols. I, II, III, 4th Ed., American Petroleum Institute, Washington, D.C., 1983.
17. Kinsler, L. E. and Frey, A. R., *Fundamentals of Acoustics,* John Wiley & Sons, New York, 3rd Ed., 1982, Chapters 9–10.
18. Wachel, J. C., "Design Audits," *Proceedings of the Fifteenth Turbomachinery Symposium,* November 1986, pp. 153–168.
19. Massey, I. C., "Subsynchronous Vibration Problems in High-Speed Multistage Centrifugal Pumps," *Proceedings of the Fourteenth Turbomachinery Symposium,* October 1985, pp. 11–16.
20. Childs, D. W. "Finite Length Solution for Rotordynamic Coefficients of Turbulent Annular Seals," ASLE Transactions, *Journal of Lubrication Technology,* 105, July 1983, pp. 437–445.
21. Karassik, Igor, "Centrifugal Pump Construction," Section 2.2, *Pump Handbook,* 2nd Ed., McGraw-Hill, 1986, pp. 2–69.
22. Childs, D. W. and Scharrer, J. K., "Experimental Rotordynamic Coefficient Results for Teeth-on-Rotor and Teeth-on-Stator Labyrinth Gas Seals," ASME Paper No. 86-GT-12, 1986.
23. Iwatsubo, T., Yang, B. and Ibaraki, R., "An Investigation of the Static and Dynamic Characteristics of Parallel Grooved Seals," The Fourth Workshop of Rotordynamic Instability Problems in High-Performance Machinery, Turbomachinery Laboratories, Texas A&M University, College Station, Texas, June 1986.
24. Black, H. F. and Jenssen, D. N., "Dynamic Hybrid Properties of Annular Pressure Seals," ASME Paper 71-WA/FF-38, 1971.
25. Wachel, J. C., and Szenasi, F. R., et al, "Rotordynamics of Machinery," *EDI Report 86-334,* April 1986, Chapters 3–5.
26. Allaire, P. E. and Flach, R. D., "Design of Journal Bearings for Rotating Machinery," *Proceedings of 10th Turbomachinery Symposium,* December, 1981.
27. Childs, D. W., "Dynamic Analysis of Turbulent Annular Seals based on Hirs' Lubrication Equation," ASME Transaction, *Journal of Lubrication Technology,* 105, July 1983, pp. 429–436.
28. Childs, D. W. and Kim, C. H., "Analysis and Testing for Rotordynamic Coefficients of Turbulent Annular Seals with Different, Directionally-Homogeneous Surface-Roughness Treatment for Rotor and Stator Elements," ASME paper, ASME-ASLE Joint Lubrication Conference, October 1984.
29. Black, H. F., "Effects of Hydraulic Forces in Annular Pressure Seals on the Vibrations of Centrifugal Pump Rotors," *Journal of Mechanical Engineering Science,* 11, (2), 1969.
30. Childs, D. W. and Moyer, D. S., "Vibration Characteristics of the HPOTP of the SSME," ASME Paper 84-GT-31,1984.
31. Von Pragenau, G. L., "Damping Seals for Turbomachinery," NASA TP-1987, March 1982.
32. Bolleter, U., Frei, A. and Florjancic, D., "Predicting and Improving the Dynamic Behavior of Multistage High Performance Pumps," *Proceedings of the First International Pump Symposium,* May 1984, pp. 1–8.
33. Wachel, J. C., "Rotor Response and Sensitivity," *Proceedings Machinery Vibration Monitoring and Analyses,* Vibration Institute, Houston, Texas, April 1983, pp. 1–12.
34. ASA STD2-1975 "Balance Quality of Rotating Rigid Bodies," Acoustical Society of American Standard, ANSI S2, 1975.
35. API Standard 617 "Centrifugal Compressors for General Refinery Services," Section 2.8, 5th Ed., American Petroleum Institute, Washington, D.C., 1988.
36. Wachel, J. C., "Rotordynamics Instability Field Problems," Second Workshop on Rotordynamic Instability of High Performance Turbomachinery, NASA Publication 2250, Texas A&M University, May 1982.
37. Black, H. F., "Calculation of Forced Whirling and Stability of Centrifugal Pump Rotor Systems," ASME Paper No. 73-DET-131, 1973.

38. Barrett, L. E., Gunter, E. J. and Nicholas, J. C., "The Influence of Tilting Pad Bearing Characteristics on the Stability of High Speed Rotor-Bearing Systems," *Topics in Fluid Film Bearing and Rotor Bearing Systems, Design and Optimization,* ASME Publication Book No. 100118, 1978, pp. 55–78.
39. Szenasi, F. R. and Von Nimitz, W., "Transient Analysis of Synchronous Motor Trains," *Proceedings of the Seventh Turbomachinery Symposium,* December 1978, pp. 111–117.
40. Szenasi, F. R. and Blodgett, L. E., "Isolation of Torsional Vibrations in Rotating Machinery," *National Conference on Power Transmissions,* 1975, pp. 262–286.
41. Military Standard 167, Bureau of Ships, 1964.
42. Peterson, R. E. *Stress Concentration Factors,* John Wiley and Sons, 1974, pp. 245– 253.
43. Frej, A., Grgic, A., Heil, W. and Luzi, A., "Design of Pump Shaft Trains Having Variable-Speed Electric Motors," *Proceedings of the Third International Pump Symposium,* May 1986, pp. 33–44.
44. Frank, K., "Frequency Converters for Starting and Speed Regulations of AC Motors for Turbomachine Applications," *Proceedings of the Tenth Turbomachinery Symposium,* December 1981, pp. 87–94.
45. Szenasi, F. R., "Diagnosing Machinery-Induced Vibrations of Structures and Foundations," ASCE Spring Meeting, April 29, 1986.
46. Wachel, J. C., "Prevention of Pump Problems," Worthington 2nd Technical Pump Conference, October 1981.
47. Allaire, P. E., et al., "Aerodynamic Stiffness of an Unbounded Whirling Centrifugal Impeller with an Infinite Number of Blades," *Workshop on Rotordynamic Instability,* Texas A&M University, May 1982.
48. Wilson, W. D., "Speed of Sound in Distilled Water as a Function of Temperature and Pressure," *Journal of the Acoustical Society of America,* Vol. 31, No. 8, August 1959, pp. 1067–1072.
49. Hayward, A. T. J., "How to Estimate the Bulk Modulus of Hydraulic Fluids," *Hydraulic Pneumatic Power,* January 1970, p. 28.
50. *Technical Data Handbook-Petroleum Refining,* Vol. I, 4th Ed., 8th Revision, American Petroleum Institute, Washington, D.C., 1983, pp. 6-65 to 6-82.

Part 4

Extending Pump Life

CENTRIFUGAL PUMPS
Design & Application
Second Edition

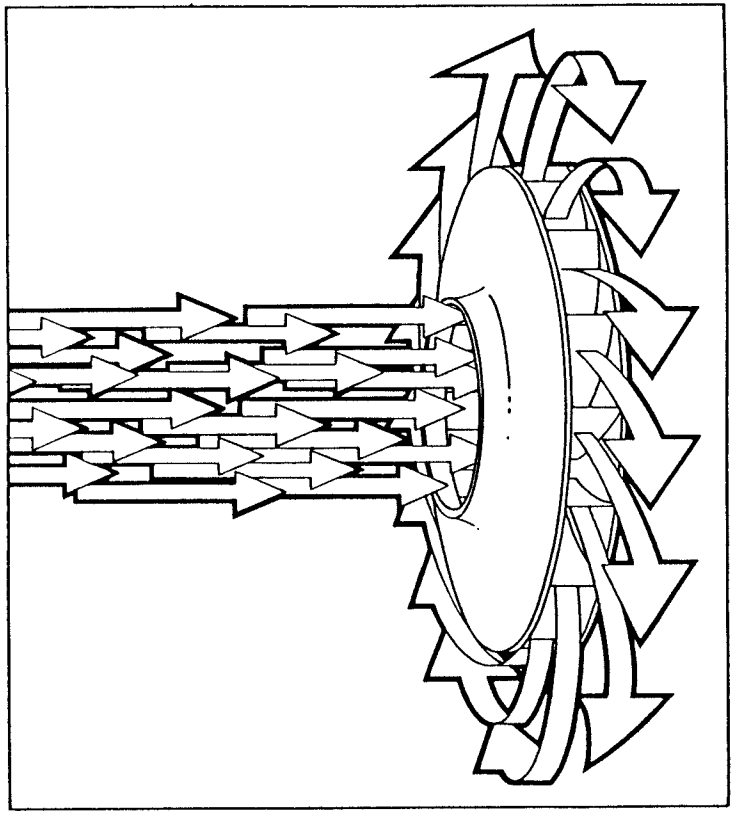

Val S. Lobanoff
Robert R. Ross

CENTRIFUGAL PUMPS
Design & Application
Second Edition

Gulf Publishing Company
Book Division
P.O. Box 2608, Houston, Texas 77252-2608

Printed on Acid-Free Paper (∞)

10 9 8 7 6 5 4 3 2 1

Library of Congress Cataloging-in-Publication Data

Lobanoff, Val S., 1910—
Centrifugal pumps: design & application/Val S. Lobanoff, Robert R. Ross.—2nd ed.
p. cm.
Includes index.
ISBN 0-87201-200-X
1. Centrifugal pumps. I. Ross, Robert R., 1934- . II. Title.
TJ919.L52 1992
621.6'7—dc20 91-41458
CIP